https://doi.org/10.5194/wes-2023-2
Preprint. Discussion started: 17 February 2023

eawe european academy of wind energy
Open Access WIND ENERGY SCIENCE DISCUSSIONS

Potential of Dynamic Wind Farm Control by Axial Induction in the Case of Wind Gusts

Florian Bürgel[1], Robert Scholz[2], Christian Kirches[1], and Sebastian Stiller[1]

[1]TU Braunschweig, Institute for Mathematical Optimization, Universitätsplatz 2, 38106 Braunschweig, Germany
[2]University of Heidelberg, Interdisciplinary Center for Scientific Computing, Im Neuenheimer Feld 205, 69120 Heidelberg, Germany

Correspondence: Florian Bürgel (f.buergel@tu-braunschweig.de)

Abstract. Wind turbines organized in wind farms will be one of the main electric power sources of the future. Each wind turbine causes a wake with a reduced wind speed. This wake influences the power of downstream turbines. Therefore, there is a strong interaction between the individual wind turbines in a wind farm. This interaction is an opportunity for optimal control to maximize the total power and decrease the load (i.e., tower activity and pitch activity) of a wind farm. We use the already known axial-induction-based control but investigate its potential in the case of a wind gust using mathematical optimization. This case is particularly interesting because a wind gust requires a dynamic control reaction and the consideration of the time delay with which downstream turbines are affected. In particular, this enables to reduce the tower load of downstream wind turbines by dynamic axial-induction-based control of an upstream turbine.

Keywords. Wind Farm, Dynamic Wake, Optimization, Axial-Induction-Based Control, Wind Gust.

1 Introduction

Wind turbines are one of the most important electric power plants of the future energy grid, since they offer energy at low costs and low green house emissions, see, e.g., Kost et al. (2018). They are among low-carbon and renewable energy. Therefore, they are a key solution against climate change. The state of the art control is that each wind turbine maximizes its own power output (greedy control) while taking care of of its own durability, see, e.g., Hau (2013). However, wind turbines are usually located in wind farms (onshore or offshore) and interact with each other. This is due to the wake caused by each wind turbine by extracting energy from the airflow. In the wake the wind speed is decreased and the turbulence is increased. Of course, this influences the power of downstream wind turbines. The local control of a wind turbine influences the length and the spatial distribution of its wake. Therefore, a greedy control strategy, which maximizes the power of each wind turbine individually, might lead to a suboptimal total power of the complete wind farm. This is an opportunity for optimal control.

Wind Farm Layout. A profitable wind farm starts with the planning. Wind farm layout optimization relies on the yearly wind frequency data (of wind direction and wind speed). It has been known for decades that it is useful to avoid the power reduction of downstream wind turbines. First attempts did not optimize, but simulated the annual average output, see Katic et al. (1987).

https://doi.org/10.5194/wes-2023-2
Preprint. Discussion started: 17 February 2023

eawe european academy of wind energy
Open Access WIND ENERGY SCIENCE DISCUSSIONS

This allocation problem can be globally solved by mixed integer programs and constraint programs, see Zhang et al. (2014). In addition to the annual energy production, the noise propagation is a topic in the case of onshore wind farms and can be taken into account, see Zhang et al. (2014). In the case of offshore wind farms, cable routing and jacket foundations are worth including in the optimization, see Fischetti and Pisinger (2019).

Wind Farm Operation. If the wind turbines are already allocated, it is state of the art that they run greedy for itself during operation, see, e.g., Hau (2013). This is done by a local wind turbine controller. The motivation of wind farm-wide control concepts is to increase the total power of the wind farm while reducing physical loads (e.g., tower load, blade load). There are two control concepts: axial-induction-based (i.e., control the generator torque and/or the collective blade pitch angle) and yaw-based (i.e., control the yaw angle), see Gebraad et al. (2015).

We consider the two control concepts in the case of two wind turbines, one of which is in the wake of the other. The first control concept (axial-induction-based) reduces the power of the regarding wind turbine, which increases the wind speed in the wake (in comparison to greedy control) and therefore increases the power of the downstream turbine. (The corresponding axial induction factor is the fractional decrease in wind velocity between free-stream and turbine rotor, see (Annoni et al., 2016, Sect. 2).) The second control concept (yaw-based) decreases the power of the regarding wind turbine, deflects the wake and increases the power of the downstream turbine. So, in both cases the upstream wind turbine outputs less power, the downstream one outputs more power. If the profit is greater than the loss, this is intended as the total power is increased. However, it depends on the allocation of the wind turbines, their characteristics and atmospheric conditions whether a control (different from greedy) is purposeful. For example, it is not possible if the wind speed is so high that both wind turbines can output their maximum power. In addition, there are cases where axial-induction-based control has no positive effect of total power but yaw-based control has a significant one, see the high-fidelity computational fluid dynamics (CFD) simulations to generator torque, collective blade pitch angle and yaw angle in Gebraad et al. (2015).

Therefore, it is consequent to combine optimal wind farm layout and yaw control as in Fleming et al. (2016); Gebraad et al. (2017). Yaw-based control is considered in Gebraad et al. (2014) (they call it game-theoretic approach), but note that it is a slow approach to a solution. However, yaw-based control does not make sense in the case of a wind gust for mechanical reasons: Due to the mechanical load, it is useful to avoid continuous small yaw movements, see Hau (2013). In addition, the yawing rate must be slow (approximately $0.5\,^\circ\,\mathrm{s}^{-1}$) to avoid gyroscopic moments, see Hau (2013).

Therefore, we focus on axial-induction-based control. The optimization in Gebraad and Wingerden (2015) deals with varying incoming wind speed and considers the annual energy while keeping physical loads in limits. However, the change of the wind speed is very slow—the method is not suitable to deal with an immediately nonsmooth wind gust. In this paper we want to overcome this limit and provide an offline optimization to investigate the potential of dynamic wind farm control. Of course, the next challenge is a real-time online optimization.

Loads. For durability reasons, it is useful to keep an eye on the physical loads of the wind turbine: the most important is the tower load. In addition, changing the pitch angle results in some wear and there is a blade load, which we do not consider. We substitute the tower load and the pitch angle changes by tower activity and pitch activity. The result of a field study, see Ennis

https://doi.org/10.5194/wes-2023-2
Preprint. Discussion started: 17 February 2023

eawe european academy of wind energy
Open Access WIND ENERGY SCIENCE DISCUSSIONS

et al. (2018), is that a slightly mathematical positive yaw offset (the exact location depends on level of shear) is best for blade load.

Models. High-fidelity simulations of wind farms in 3D are impractical for control. An overview of the most important control-oriented models[1] in 2D is given in (Annoni et al., 2018, Sect. 2.1): it includes the Jensen model, see Jensen (1983); Katic et al. (1987) for a further developed model, the multi-zone model FLORIS, see Gebraad et al. (2014),—the dynamic extension is FLORIDyn, see Gebraad and van Wingerden (2014),—and the Gaussian model, see, e.g., Bastankhah and Porté-Agel (2016). To give a classification, we use a model that bases on FLORIDyn.

We consider NREL 5-MW wind turbines, see Jonkman et al. (2009) for technical details, in usual atmospheric conditions for onshore wind farms, see Sect. 2.1 for details.

However, we should keep in mind that these control-oriented models have limitations: In the case of specific atmospheric conditions, wakes of offshore wind farms can have a length of 45 km in real-world, see Platis et al. (2018). Such special cases are explicitly excluded.

In addition, if pitch angle or generator torque have an offset, there is a discrepancy between control-oriented model (FLORIS, see Gebraad et al. (2016)) and high-fidelity simulation (SOWFA, see National Renewable Energy Laboratory (NREL) (2020)) (for NREL 5-MW wind turbines), see Annoni et al. (2016).[2] It also explains the background of axial-induction-based control and suggests the FLORIS-vk_e3 model to reduce the discrepancy. The model chooses the wake expansion coefficient k_e in dependence of the axial induction factor and three fitting parameters. However, we use the simulation software WinFaST[3], see Sect. 2.1 for a short description, that bases on FLORIDyn as described in Gebraad and van Wingerden (2014), i.e., it uses a fixed expansion coefficient. We emphasize at this point that in Annoni et al. (2016) averaged wind speed with turbulence is considered and a fixed control over time is used, whereas we consider wind gusts and a dynamic control.

Goal. The goal of this paper is to investigate the potential of axial-induction-based dynamic control in the case of a wind gust to increase the power and decrease the load. This case is particularly interesting because a wind gust requires a dynamic control reaction and the consideration of the time delay with which downstream turbines are affected, i.e., we have to deal with a strong transient behavior. As we know the wind speed a priori, it is an offline optimization. However, this provides an impression of the potential of real-time online optimization. To do this proof of concept, we use error free simulation data and do not pay particular attention to the run time. Besides the expected increase in total power, we point out the option to reduce the tower load of downstream wind turbines by dynamic axial-induction-based control of an upstream turbine. To the best of

[1] They are also called *engineering models*.

[2] Without offset, i.e., at the maximum operating point, there is no significant discrepancy between the results from models. With offset there might be one (at least for the considered offshore conditions) that effects the total power: They carefully describe in the conclusions that the simulation examples suggest the existence of circumstances where axial-induction-based control can not increase the total power of the wind farm, see (Annoni et al., 2016, Sect. 7). (It is worth noting that their simulated conditions represent an almost ideal case for axial-induction-based control, see the scenario with two turbines in (Annoni et al., 2016, Sect. 5.1.2).) We have already mentioned Gebraad et al. (2015) above with an analogous statement. However, the use of the high-fidelity model is not an alternative for control as the high-fidelity simulations took them days of run time on a supercomputer, see (Annoni et al., 2016, Sect. 3.2).

[3] The MATLAB software package WinFaST, which stands for *Wind Farm Simulation Tool*, was written by Bastian Ritter and Thorsten Schlicht. Within the project MOReNet the company IAV GmbH has provided us this internal company software together with the corresponding documentation.

https://doi.org/10.5194/wes-2023-2
Preprint. Discussion started: 17 February 2023

eawe european academy of wind energy
Open Access WIND ENERGY SCIENCE DISCUSSIONS

our knowledge, we are the first reducing the tower load by dynamically controlling an upstream wind turbine. In addition, we combine it with the provided option in the simulation software WinFaST to damp tower oscillations of itself.

Structure. We describe the simulation and optimization methods in Sect. 2. We explain and discuss the results of the computational experiments in Sect. 3. A final conclusion is in Sect. 4. The results and evaluations of the computational experiments themselves are available as tables in App. A. The corresponding figures are in App. B. (As abbreviations we use Eq., Sect., and Fig. for Equation, Section, and Figure.)

2 Simulation and Optimization Methods

We define the experimental set-up of our computational experiments in Sect. 2.1. We consider in Sect. 2.2 the wind farm control inputs and simulation outputs, which lead us to the objective function. We describe the optimization scenarios in Sect. 2.3 and their solution methods in Sect. 2.4.

2.1 Experimental Set-Up

Wind Farm Layout and Operation. In our experimental set-up, we will consider NREL 5-MW wind turbines with a rating value of 5 MW and a rotor diameter of 126 m, see (Jonkman et al., 2009, Table 1-1). As we are interested in the potential of axial-induction-based control, the yaw angles are fixed to a yaw offset of 0°.

We consider wind farms with $n_{\mathrm{WT}} \in \mathbb{N}$ wind turbines in a straight line in the wind direction with a distance of $5D$, where $D = 126\,\mathrm{m}$ is the rotor diameter. We will focus on the case with $n_{\mathrm{WT}} = 2$. The corresponding wind farm layout is depicted in Fig. 1. The upstream turbine is labeled WT01 and the downstream turbine WT02.

Turbulence Intensity. We always describe an average wind speed. Actually, we consider wind with turbulence, i.e., the (horizontal) ambient wind speed U_{amb}. The *turbulence intensity* I is defined as

$$I = \frac{\sigma}{\langle U_{\mathrm{amb}} \rangle},$$

where σ is the standard deviation and $\langle U_{\mathrm{amb}} \rangle$ the average of the (horizontal) ambient wind speed, see, e.g., (Hau, 2013, Sect. 13.4). This average is also denoted by U_{ave}.

Scenarios. We distinguish between three scenarios. They all have a fixed turbulence intensity of $I = 0.01$ in common.[4] Despite the turbulence we speak abbreviated of *low wind speed* or *high wind speed*. In both cases we mean a wind speed that is constant on average. Therefore, we also use the term *constant wind speeds* if we mean both cases. The third scenario is a *wind gust*. A detailed description is the following:

[4] We will always consider wind gusts with a change of $1\,\mathrm{m\,s^{-1}}$. The understanding of the choice needs an anticipation. We will consider the following wind gusts: 6–7, 11–12, 12–13 $\mathrm{m\,s^{-1}}$. The turbulence should have an effect but they should not be in the order of the wind gust itself. So, e.g., a choice of $I = 0.1$ would not make sense.

https://doi.org/10.5194/wes-2023-2
Preprint. Discussion started: 17 February 2023

WIND ENERGY SCIENCE DISCUSSIONS

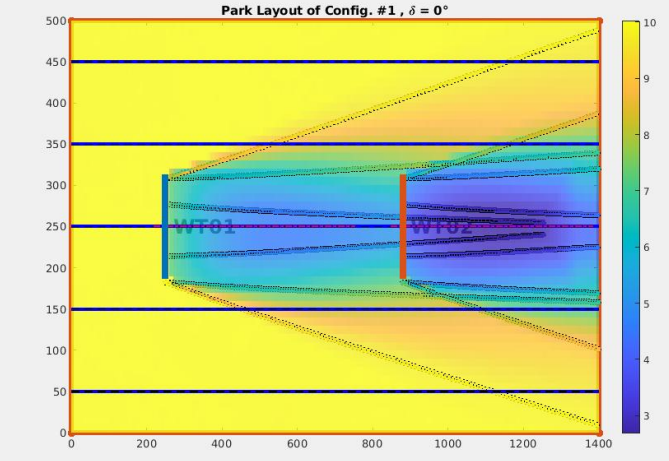

Figure 1. Example layout with two wind turbines and wind speed of $10\,\mathrm{m\,s^{-1}}$. The wind direction is depicted by the horizontal lines. The orientation is to the right. The axes describe the positions in the unit meters. The local wind speed is indicated by the color scheme (in unit $\mathrm{m\,s^{-1}}$). This figure was produced using WinFaST.

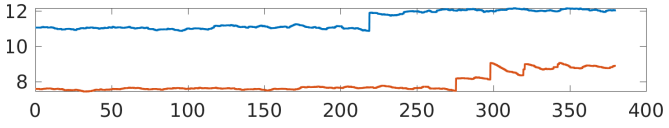

Figure 2. Example of a wind gust (with wind speed of 11–12 $\mathrm{m\,s^{-1}}$). The hub-height wind speed (in $\mathrm{m\,s^{-1}}$) of the upstream wind turbine (plotted in blue) over the time (in s) represents a part of the wind gust scenario. In general we use U_ℓ for low wind speed (constant on average), U_h for high wind speed (constant on average) and U_ℓ–U_h for the wind gust. Of course, the wind arrives at the downstream wind turbine (plotted in red) with delay and influenced by the upstream one.

- Scenario 1 (low wind speed): we consider the two turbines in the case of an average constant low wind speed of U_ℓ over the entire simulation time.
- Scenario 2 (high wind speed): we consider the two turbines in the case of an average constant high wind speed of U_h.
- Scenario 3 (wind gust): In this scenario we begin with the low wind speed U_ℓ (constant on average), such that the wake dynamics are more or less in a steady state. Then, we model a wind gust by an immediate change from U_ℓ to the high wind speed U_h (constant on average). After this, we provide enough time such that the wake dynamics are more or less in a steady state again. Fig. 2 shows an example of a wind gust. We use the abbreviated term *wind speed of 11–12* $\mathrm{m\,s^{-1}}$ to describe scenario 3 including a wind gust of 11 to 12 $\mathrm{m\,s^{-1}}$.

Steady States and Transient Phase. For more or less constant wind conditions and constant controls (apart from reactions to turbulence), the wind farm settles to a state, that we consider as *steady state*. This is the case for scenarios 1 and 2.

https://doi.org/10.5194/wes-2023-2
Preprint. Discussion started: 17 February 2023

eawe european academy of wind energy
Open Access WIND ENERGY SCIENCE DISCUSSIONS

A change of wind conditions or controls influences the wake. The effect propagates downstream and reaches downstream wind turbines with a time delay. So, the system is in a *transient phase* until all effects are propagated though the complete wind farm. In scenario 3 the system is in a transient phase.

Time Intervals. We denote the *simulation time interval* by $[t_{\mathrm{s}_1}, t_{\mathrm{s}_2}]$. Typically, $t_{\mathrm{s}_1} = 0$. Basically, both wind turbines are controlled by the local standard controller. In addition, we influence the controller of the upstream wind turbine within simulation time. Within this *full control time interval* we chose a smaller *dynamic control time interval*, $[t_{\mathrm{c}_1}, t_{\mathrm{c}_2}]$, for dynamic control to react on wind gust. The dynamic control time interval will be chosen such that the immediate wind change reaches the upstream wind turbine in its middle and such that the control can effect the downstream wind turbine within the simulation time interval. We leave out the details. For data analysis we choose an *observation time interval*, $[t_{\mathrm{o}_1}, t_{\mathrm{o}_2}]$, that starts before the dynamic control begins and ends so that the effect of dynamic control is definitely in the interval. Again, we leave out the details. Finally, $t_{\mathrm{s}_1} < t_{\mathrm{o}_1} < t_{\mathrm{c}_1} < t_{\mathrm{c}_2} < t_{\mathrm{o}_2} \leq t_{\mathrm{s}_2}$. Typically, $t_{\mathrm{s}_1} = 0$ and $t_{\mathrm{o}_2} = t_{\mathrm{s}_2}$. All time intervals are in $\mathbb{R}$ and have the unit s. An example is given in Fig. 3.

In Summary, we have the following time intervals:

- $[t_{\mathrm{s}_1}, t_{\mathrm{s}_2}]$ Simulation time interval (as well as full control time interval)
- $[t_{\mathrm{c}_1}, t_{\mathrm{c}_2}]$ Dynamic control time interval
- $[t_{\mathrm{o}_1}, t_{\mathrm{o}_2}]$ Observation time interval

Simulation Software. As already mentioned in Sect. 1, we use the MATLAB software package WinFaST for simulation. For orientation we give a short description.

We have to fix the wind farm layout before starting the simulation. Out of the box, individual parameters for axial induction (set by a power reference value) and yaw angles are possible. The modular structure of the package—it uses the modelling framework Simulink—enables modifications for the targeted individual axial-induction-based control. The modular structure of the software would even allow a replacement of the wind turbine controller.

The dynamic wake model relies on FLORIDyn, see Gebraad and van Wingerden (2014). As already mentioned, FLORIDyn is the dynamic extension of the multi-zone model FLORIS, see Gebraad et al. (2014). It uses more wake zones (7 instead of 3 in FLORIS). Further, so-called observation points are defined to compute local wake characteristics. In addition, wake interaction bases on Katic et al. (1987), see (Gebraad and van Wingerden, 2014, Sect. 2).

The controller in WinFaST relies on Jonkman et al. (2009), which is more or less the standard industrial wind turbine controller, but was extended by the options to reduce the power and damp tower oscillations (of itself).[5] There is no individual pitch control activated, i.e., all blades of a turbine have collectively the same pitch angle.

[5] Both options were developed as part of WinFaST.

https://doi.org/10.5194/wes-2023-2
Preprint. Discussion started: 17 February 2023

eawe european academy of wind energy
Open Access WIND ENERGY SCIENCE DISCUSSIONS

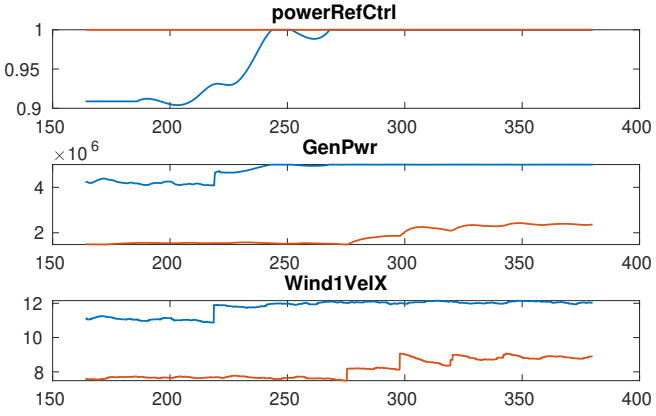

Figure 3. Example of control time intervals. For the example we anticipate parts of Fig. 5, which considers a wind gust (11–12 $\mathrm{m\,s^{-1}}$). The quantity Wind1VelX is the hub-height wind speed in $\mathrm{m\,s^{-1}}$. All quantities are depicted over the time in s, which we restrict in the plot to the observation time interval, e.g., $[t_{\mathrm{o}_1}, t_{\mathrm{o}_2}] = [164, 380]$. The quantities for the upstream wind turbine are depicted in blue and for the downstream one in red. The quantity powerRefCtrl is the power reference value, which we control in the dynamic control time interval, e.g., $[t_{\mathrm{c}_1}, t_{\mathrm{c}_2}] = [186, 268]$, and GenPwr is the generator power in W, which we analyze in the observation time interval. The simulation time interval (as well as the full control time interval) is $[t_{\mathrm{s}_1}, t_{\mathrm{s}_2}] = [0, 380]$ in this example. (A detailed explanation of the quantities follows in Sect. 3.1. More examples of time intervals are given in Table 2.)

Simulation Software. The software WinFaST uses the same parametric model parameters for turbine and wake as in (Gebraad and van Wingerden, 2014, Table 1) with the exception of the air density, that is set to 1.225 $\mathrm{kg\,m^{-3}}$ as in (Jonkman et al., 2009, App. B.1).

2.2 Wind Farm Control

The software WinFaST uses a hierarchical control structure. Every turbine is equipped with a local wind turbine controller, which reacts to local measurements. The control strategy of each individual standard wind turbine controller is to run greedy, i.e., to maximize the power of each wind turbine (regardless of the total power of the wind farm) but to preserve the turbine from physical damage. However, the local controllers in WinFaST can take into account reference values from a centralized wind farm controller in order to determine control targets. Since we are interested in wind farm control, we use the reference values to influence the turbines.

Control Inputs. The package WinFaST provides three reference vectors as control inputs:

- The *yaw reference* $u_\gamma \in [-180, 180]^{n_{\mathrm{WT}}}$ in the unit degrees controls the *yaw angle* relative to the wind direction.
- The *power reference* $u_{\mathrm{p}} \in [0.5, 1]^{n_{\mathrm{WT}}}$ controls the *power factor* of the turbines. Depending on the working condition, it influences the axial induction by generator torque and/or blade pitch angle.

https://doi.org/10.5194/wes-2023-2
Preprint. Discussion started: 17 February 2023

eawe european academy of wind energy
Open Access WIND ENERGY SCIENCE DISCUSSIONS

Table 1. Notation of control inputs.

Quantity	Source code vector	Symbol of vector	Symbol of value
Yaw reference	yawRef	u_γ	$u_{\gamma,\mathrm{v}}$
Power reference	powerRef	u_p	$u_{\mathrm{p,v}}$
Fatigue reference	fatigueRef	u_f	$u_{\mathrm{f,v}}$

– The *fatigue reference* $u_\mathrm{f} \in [0,1]^{n_\mathrm{WT}}$ enables active tower damping, i.e., it reduces the tower load, in that it damps the tower oscillations. Since we only make it either off or on, we use the expressions *without/with fatigue reduction*.

The corresponding notation in the source code is yawRef, powerRef and fatigueRef.[6] Note that these three references are vectors, e.g. yaw reference $u_\gamma = (0,0)^\mathrm{T}$ in the case of two wind turbines. The corresponding entry for a specific wind turbine is called *reference value*: yaw, power and fatigue reference values are denoted by $u_{\gamma,\mathrm{v}}$, $u_{\mathrm{p,v}}$ and $u_{\mathrm{f,v}}$. The notation is summarized in Table 1.

Control Function. Out of the box WinFaST enables fixed control inputs for the full simulation time interval. However, the Simulink model can be modified such that time-dependent control inputs are possible. In particular, we only modified it in the case of the power reference. However, we define the control function in dependence of the time for all three control inputs.

$$u\colon [t_{\mathrm{s}_1}, t_{\mathrm{s}_2}] \to ([-180,180]^{n_\mathrm{WT}}, [0.5,1]^{n_\mathrm{WT}}, [0,1]^{n_\mathrm{WT}}), \quad t \mapsto (u_\gamma, u_\mathrm{p}, u_\mathrm{f}), \tag{1}$$

where u_γ, u_p and u_f are column vectors.

Simplified Control Function. We will discuss some simplifications that will lead to a simplified control function.

– First, as already mentioned, the yaw movement causes a high physical load and is therefore adjusted with a low sampling rate (for example every 15 min). Since we are interested in the dynamic effects of a high frequency control, we do not consider yaw control in this paper. Therefore, its reference is kept constant over the complete simulation time interval (to a yaw offset of 0).

– Second, the fatigue reference enables active tower damping in the local wind turbine controllers. In this paper, we consider either without or with fatigue reduction, i.e., $u_{\mathrm{f,v}} \in \{0,1\}$. Furthermore, the fatigue reference value will be fixed during the optimization.

– Third, the wake dynamics are only affecting downstream turbines and therefore the downstream-most turbine is not affecting any other turbine. Therefore we assume, that the downstream-most turbine is controlled in a greedy way, i.e., it

[6] In WinFaST itself the names are info.IV_PowerRef, info.IV_YawRef, info.IV_FatigueRef. They do not mean exactly the same: in the case of the yaw reference we mean the angle relative to the wind direction and WinFaST means the absolute direction.

https://doi.org/10.5194/wes-2023-2
Preprint. Discussion started: 17 February 2023

eawe european academy of wind energy
Open Access WIND ENERGY SCIENCE DISCUSSIONS

maximizes its own power using the power reference value of 1. The power reference value of the upstream turbines can be changed during the *full control time interval*, which coincides with the *simulation time interval*, see Sect. 2.1.

- Fourth, we will consider a wind farm with $n_{\mathrm{WT}} = 2$ wind turbines.

All in all, the simplified control function of our upstream wind turbine is

$$u_* \colon [t_{\mathrm{s}_1}, t_{\mathrm{s}_2}] \to [0.5, 1], \quad t \mapsto u_{\mathrm{p,v}}. \tag{2}$$

Regardless of the defined function u_*, we refer in subscripts only to u. As already mentioned, dynamic control (to react on a wind gust) is only done in the smaller *dynamic control time interval* $[t_{\mathrm{c}_1}, t_{\mathrm{c}_2}]$.

In order to be suitable for numerical optimization methods, we need a parametrization of the control function. This parametrization depends on the scenario and we will discuss it in Sect. 2.4.

Simulation Outputs. We have two main objectives when controlling the wind farm: maximizing the total electrical energy output and minimizing the physical load of the turbines. Typically, these are conflicting objectives. Therefore, our objective function Eq. (3) will be a weighted sum of different performance indicators, which in themselves consist of the following three outputs of WinFaST. (They all depend on the control function u and the time. Remember that we receive data over the entire simulation time interval $[t_{\mathrm{s}_1}, t_{\mathrm{s}_2}]$, but we only analyze results in the observation time interval $[t_{\mathrm{o}_1}, t_{\mathrm{o}_2}]$.)

- The *power* of each wind turbine is given in the unit W as function

  $$p_u \colon [t_{\mathrm{s}_1}, t_{\mathrm{s}_2}] \to \mathbb{R}_{\geq 0}^{n_{\mathrm{WT}}}.$$

- The tower load is high, when the nacelle is oscillating. Therefore, we use the *velocity of the nacelle* in unit $\mathrm{m\,s^{-1}}$ in wind direction

  $$v_u \colon [t_{\mathrm{s}_1}, t_{\mathrm{s}_2}] \to \mathbb{R}^{n_{\mathrm{WT}}}.$$

- The pitch rate should be kept within limits because of the load of the pitch actuators. Therefore, we use the *blade pitch angle* in the unit degree

  $$\beta_u \colon [t_{\mathrm{s}_1}, t_{\mathrm{s}_2}] \to \mathbb{R}^{n_{\mathrm{WT}}}.$$

We explicitly do not consider the blade load as WinFaST does not provide a suitable output quantity.

Performance Indicators. For our objective function we will consider three performance indicators for the whole wind farm: the power, the tower activity and the pitch activity. For the last two we consider the nacelle velocity v and the blade pitch angle β. All three quantities are averages over the observation time interval $[t_{\mathrm{o}_1}, t_{\mathrm{o}_2}]$. As the wind farm is viewed holistically, we denote the functions by h_{p}, $h_{\mathrm{a_T}}$ and $h_{\mathrm{a_P}}$.

https://doi.org/10.5194/wes-2023-2
Preprint. Discussion started: 17 February 2023

eawe european academy of wind energy
Open Access WIND ENERGY SCIENCE DISCUSSIONS

– For the average *power* in the unit MW we compute

$$P := h_{\mathrm{p}}(u) := \sum_{i=1}^{n_{\mathrm{WT}}} \frac{1}{t_{\mathrm{o}_2} - t_{\mathrm{o}_1}} \int_{t_{\mathrm{o}_1}}^{t_{\mathrm{o}_2}} 10^{-6} \, (p_u(t))_i \, \mathrm{d}t.$$

Note that we divide by 10^6 to receive a result in the unit MW instead of W.

– An oscillating nacelle results in a high tower load. So, we use the absolute value of the velocity of the nacelle (in wind direction) to estimate the tower load by the so-called *tower activity*

$$a_{\mathrm{T}} := h_{\mathrm{a_T}}(u) := \sum_{i=1}^{n_{\mathrm{WT}}} \frac{1}{t_{\mathrm{o}_2} - t_{\mathrm{o}_1}} \int_{t_{\mathrm{o}_1}}^{t_{\mathrm{o}_2}} |(v_u(t))_i| \, \mathrm{d}t.$$

The unit of the tower activity is $\mathrm{m\,s^{-1}}$ but has no physical meaning.

– Similarly, we use the absolute value of the velocity of the blade pitch angle to estimate the load of the pitch actuators by the so-called *pitch activity*

$$a_{\mathrm{P}} := h_{\mathrm{a_P}}(u) := \sum_{i=1}^{n_{\mathrm{WT}}} \frac{1}{t_{\mathrm{o}_2} - t_{\mathrm{o}_1}} \int_{t_{\mathrm{o}_1}}^{t_{\mathrm{o}_2}} \left| \frac{\mathrm{d}}{\mathrm{d}t} (\beta_u(t))_i \right| \mathrm{d}t.$$

The unit of the pitch activity is $^\circ\,\mathrm{s^{-1}}$ but has no physical meaning.

Objective Function. The objective function, which we will minimize, combines these three performance indicators in a weighted sum with the parameters $\omega = (\omega_{\mathrm{T}}, \omega_{\mathrm{P}}) \in \mathbb{R}^2_{\geq 0}$ in dependence of the control function:

$$f_\omega(u) := -h_{\mathrm{p}}(u) + \omega_{\mathrm{T}} \, h_{\mathrm{a_T}}(u) + \omega_{\mathrm{P}} \, h_{\mathrm{a_P}}(u). \tag{3}$$

The weights are always chosen in a way that the main emphasis is on the power. In Sect. 3 we present computational experiments with different weights ω_{T} as well as ω_{P} and we discuss the influence of the different parts of the objective function.

We describe a case as *without/with tower activity weight* if ω_{T} is zero/non-zero. In the same sense we use the expressions *without/with pitch activity weight*.

2.3 Optimization Scenarios

We briefly describe our optimization scenarios and their connection before the methods follow in Sect. 2.4.

Optimization Scenarios. The scenarios we optimize are the same as in Sect. 2.1: in scenario 1 we consider a low wind speed U_ℓ, in scenario 2 a high wind speed U_{h}, and in scenario 3 a wind gust from U_ℓ to U_{h}. Remember that the wind speeds in

https://doi.org/10.5194/wes-2023-2
Preprint. Discussion started: 17 February 2023

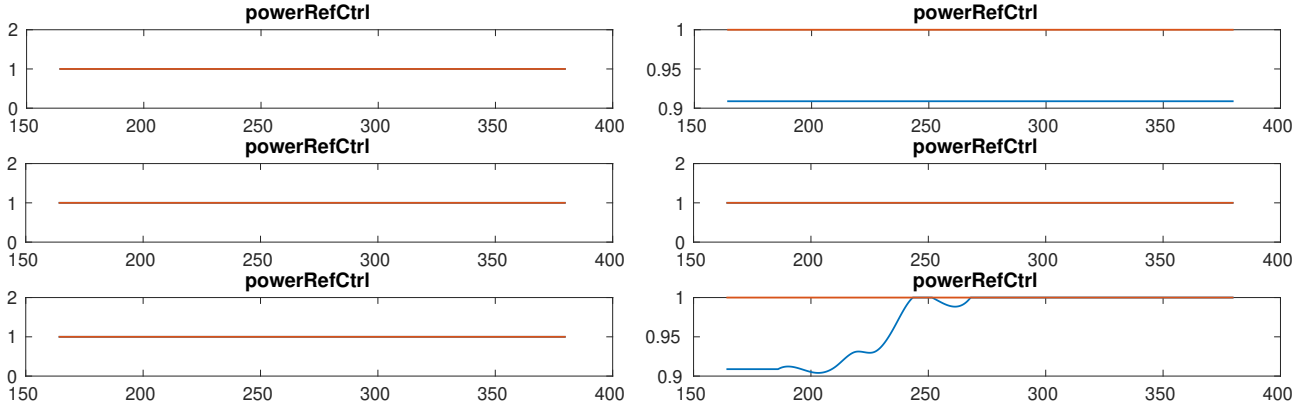

(a) Scenarios 1–3 baseline.

(b) Scenarios 1–3 optimization.

Figure 4. Baseline and optimization output for scenarios 1–3 (for test series 1 case 5). All figures show the power reference values over the simulation time (in s). We restrict the time to the observation time interval. The power reference value of the upstream wind turbine is blue and of the downstream wind turbine red. (A detailed explanation of such figures is in Sect. 3.1.) (a) In the baseline simulation all power reference values are 1. (b) In the optimization, the power reference value of the upstream wind turbine can be lower than 1. Note that control in optimization can be the same as in baseline; scenario 2 is an example. In the optimization of scenario 3, the downstream wind turbine is controlled greedy and the upstream wind turbine more sophisticated, i.e., in the dynamic control time interval by cubic spline interpolation (within limits of power reference control) and outside this interval by fixed values (from steady state optimization). For the details of the optimization methods, we refer to Sect. 2.4.

scenarios 1 and 2 are constant on average, i.e., we have turbulence but no wind gust. However, in this cases the wind farm is more or less in a steady state. In contrast, in scenario 3, the wind farm is first in a steady state (as in scenario 1), then in a dynamic state (caused by the wind gust), and then in a steady state again (this time as in scenario 2).

Connection of the Scenarios. Therefore, it is useful to start with the optimizations of scenarios 1 and 2 (steady state optimizations) and recycle the resulting optimal controls, i.e., the reference values p_ℓ (from low wind scenario 1) and p_h (from high wind scenario 2), in the optimization of scenario 3. This reduces the requirement of a continuous control function (to react to the transient behavior) to the dynamic control time interval $[t_{\mathrm{c}_1}, t_{\mathrm{c}_2}]$. Outside this time interval, the reference values are fixed to p_ℓ and p_h. In this context, it is worth remembering that the observation interval $[t_{\mathrm{o}_1}, t_{\mathrm{o}_2}]$ is chosen such that the effect of the dynamic control is completely captured.

Baseline and Optimization Output. For each scenario we will consider two cases: first, we run a baseline simulation, i.e., without optimization; second, we run the simulation with optimization solution. The comparison of these outputs allows us to make a statement about the potential of the optimal control. For a first impression, Fig. 4 shows the power reference values over the time for baseline and optimization output. A detailed discussion of the potential is in Sect. 3.

https://doi.org/10.5194/wes-2023-2
Preprint. Discussion started: 17 February 2023

eawe european academy of wind energy
Open Access WIND ENERGY SCIENCE DISCUSSIONS

2.4 Optimization Methods

First, we consider the optimization problems in dependence of the scenarios, divided into steady states and dynamic state. Second, we discuss numerical aspects.

2.4.1 Steady State Optimization Method

The aim of the steady state optimization is to compute optimal power reference values $u_{\mathrm{p,v}}$ for all $n_{\mathrm{WT}} - 1$ upstream wind turbines in a steady state scenario, i.e., constant wind speed on average. We remember that the downstream-most wind turbine is fixed to greedy control, i.e., $u_{\mathrm{p,v}} = 1$.

WinFaST Simulation. The simulation in WinFaST works in two steps: First, it computes a *WinFaST steady state simulation* for a fixed wind farm layout, fixed wind conditions and fixed control inputs. This is necessary to set the so-called tracking points. Second, it runs the *actual simulation*, in which control inputs can be modified. For reasons of run time, it is best practice to recycle this WinFaST steady state simulation. (Note that this steady state describes a technical steady state and has a different meaning than the described steady state scenarios 1 and 2.)

For the WinFaST steady state simulation, we always use yaw reference values of $u_{\gamma,\mathrm{v}} = 0$, power reference values of $u_{\mathrm{p,v}} = 1$ and fatigue reference values of $u_{\mathrm{f,v}} = 0$. For the actual simulation, we might change our control inputs. In fact, we remain the yaw reference values, might change the power reference values of the upstream wind turbines to other fixed values and might change the fatigue reference values.

Observation Time Interval. In the case of a change we have to deal with a disadvantage of these two steps of WinFaST: there is a transient phase in the actual simulation as we have to change from the control of the initial WinFaST steady state simulation to a new steady state of the applied control in the actual simulation. Therefore, we choose the observation time interval such that this transient phase is outside.

Optimization Problem. We remind the objective function f_ω, see Eq. (3), and the simplified control function u_*, see Eq. (2). As already mentioned, in the steady state optimization all control inputs are fixed over the simulation time interval.

Finally, we solve two steady state optimization problems. First, for the low wind speed (scenario 1)

$$\begin{aligned} \min_{p_\ell} \quad & f_\omega(u_*) \\ \text{s.t.} \quad & u_*(t) = p_\ell, \quad t \in [t_{\mathrm{s}_1}, t_{\mathrm{s}_2}], \end{aligned} \tag{4}$$

where p_ℓ denotes the fixed power reference value of the upstream wind turbine.[7]

Second, for the high wind speed (scenario 2)

$$\begin{aligned} \min_{p_\mathrm{h}} \quad & f_\omega(u_*) \\ \text{s.t.} \quad & u_*(t) = p_\mathrm{h}, \quad t \in [t_{\mathrm{s}_1}, t_{\mathrm{s}_2}], \end{aligned} \tag{5}$$

[7]The power reference value itself was already denoted by $u_{\mathrm{p,v}}$ in Sect. 2.2. However, we use p_ℓ and p_h to distinguish the two fixed values.

https://doi.org/10.5194/wes-2023-2
Preprint. Discussion started: 17 February 2023

eawe european academy of wind energy
Open Access WIND ENERGY SCIENCE DISCUSSIONS

where p_{h} denotes the fixed power reference value of the upstream wind turbine.

Examples of the control function in steady state optimization were already depicted in scenarios 1 and 2 of Fig. 4(b).

2.4.2 Dynamic State Optimization Method

As already mentioned, in the dynamic state optimization (scenario 3), we want continuous control in the dynamic time interval $[t_{\mathrm{c}_1}, t_{\mathrm{c}_2}]$ and we use precomputed fixed optimal controls (p_ℓ and p_{h}) outside.

Discretization. The control function u, see Eq. (1), and the simplified u_*, see Eq. (2), are continuous. We need a discretization to use numerical optimization solvers. Outside the dynamic control time interval $[t_{\mathrm{c}_1}, t_{\mathrm{c}_2}]$ the function values are fixed to p_ℓ and p_{h}. For time t in $[t_{\mathrm{c}_1}, t_{\mathrm{c}_2}]$, we use a cubic spline interpolation with a number of n_{ctrl} intermediate uniform knots at $t_1, \dots, t_{n_{\mathrm{ctrl}}}$ (within $[t_{\mathrm{c}_1}, t_{\mathrm{c}_2}]$) and two boundary knots (at t_{c_1} with value p_ℓ and at t_{c_2} with value p_{h}). The boundary conditions are chosen to ensure a safe transition to the fixed part of the control function. The matrix of interpolation values (at $t_1, \dots, t_{n_{\mathrm{ctrl}}}$) is given by $\varphi \in \mathbb{R}^{n_{\mathrm{ctrl}} \times n_{\mathrm{WT}}-1}$. As we consider two wind turbines, φ is a vector. We summarize the cubic spline interpolation $S_{p_\ell, p_{\mathrm{h}}, \varphi}$ by the knots of it:

$$S_{p_\ell,p_{\mathrm{h}},\varphi} \colon [t_{\mathrm{c}_1}, t_{\mathrm{c}_2}] \to [0.5, 1], \quad S(t) := \begin{cases} p_\ell & \text{if } t = t_{\mathrm{c}_1}, \\ \varphi_i & \text{if } t = t_i \text{ for } i = 1, \dots, t_{n_{\mathrm{ctrl}}}, \\ p_{\mathrm{h}} & \text{if } t = t_{\mathrm{c}_2}. \end{cases}$$

We make attention to the limited codomain because of the codomain of the power reference, see Sect. 2.2. It turned out in computational experiments that the number of intermediate knots of $n_{\mathrm{ctrl}} = 9$ is purposeful.[8]

Optimization Problem. We remember the objective function f_ω, see Eq. (3). Finally, we solve the dynamic state optimization problem

$$\min_{\varphi} \quad f_\omega(u_*)$$

$$\text{s.t.} \quad u_*(t) = \begin{cases} p_\ell & \text{if } t_{\mathrm{s}_1} \le t \le t_{\mathrm{c}_1}, \\ S_{p_\ell,p_{\mathrm{h}},\varphi}(t) & \text{if } t_{\mathrm{c}_1} < t \le t_{\mathrm{c}_2}, \\ p_{\mathrm{h}} & \text{if } t_{\mathrm{c}_2} < t \le t_{\mathrm{s}_2}. \end{cases}$$

Of course, we have to solve the optimization problems of the steady state optimization before, i.e. Eqs. (4) and (5).

An example of the control function in dynamic state optimization was already depicted in scenario 3 of Fig. 4(b).

Wind Gust Simulation Workaround. Out of the box, the simulation software WinFaST can add turbulence but no wind gust. Remember that the WinFaST steady state simulation generates a wind field (with a desired turbulence intensity) and sets the corresponding tracking points.

[8] In our experience, 5 is too small, 7 is sometimes too small, 9 is a reasonable choice. On the other hand, 10 is too high as the modification of one intermediate value has no significant effect on the objective value.

https://doi.org/10.5194/wes-2023-2
Preprint. Discussion started: 17 February 2023

To incorporate a wind gust, we modify the wind field of the lower wind speed and run the actual simulation. Note that the tracking points are set for the original wind field, i.e., for lower wind speed—as we increase the wind speed, we can neglect this effect.

However, we carefully restrict the computational experiments to a change of $1\,\mathrm{m\,s^{-1}}$. This is a strong limitation compared to real-world wind gusts, which have greater changes.

In this context, the behavior of the wind field in the actual simulation is worth mentioning as it is pushed through the wind farm with the average wind speed of the steady state simulation. This does not negatively influence the simulation of the wind speed itself but it leads to temporal inaccuracies of the travel time, i.e., in our scenarios the wind gust consistently reaches the downstream wind turbine too early.

2.4.3 Numerical Optimization Method

The software WinFaST computes the simulation of the wind farm without any sensitivity information. Therefore, gradient-based optimization algorithms are not directly accessible. We employ the *nonlinear programming* (NLP) solver fmincon in MATLAB, which uses finite differences internally to compute gradients.

As optimization method we have chosen *sequential quadratic programming* (SQP).[9] As options we set the maximum number of iterations to 20 and the step tolerance (on the power reference value) to 0.01.[10]

Initial Power Reference Values. As SQP is a local optimization method, the result depends on the initial value(s).

For scenarios 1 and 2, i.e., low and high wind speed (both constant on average), we start with a power reference value of 1, i.e., $p_\ell = 1$ and $p_\mathrm{h} = 1$.

For scenario 3, i.e., the wind gust, preliminary computational experiments with a very slow increase of the wind speed with a global optimization method suggested to increase the power reference value analogously to the wind speed (as long as the rated wind speed, which is $11.4\,\mathrm{m\,s^{-1}}$ for the considered NREL 5-MW wind turbines, see (Jonkman et al., 2009, Table 1-1), is not reached). Of course, the time scale of the wind gust is very important, so that the preliminary experiments are not directly comparable to an immediate wind gust. However, it turned out that a reasonable initialization follows this spirit: We set the first half of entries of φ to p_ℓ and the second half of entries to p_h. In the case of an odd number of entries, the middle entry of φ is set to p_ℓ. (Remember that the dynamic control time interval is chosen such that the immediate wind change is in its middle.)

Software. The described method to find out the potential of dynamic wind farm control by axial induction is available as a module of the self-developed and unpublished *Wind Farm Optimization* software suite WiFaOpt. Remember that the simulation itself uses WinFaST.

[9] Apart from sqp, we also tried interior-point and active-set. However, they mostly stuck in a worse local minimum.

[10] In our computational experiments, a change of the third decimal in power reference did not change the fourth decimal of the power. Therefore, a step tolerance of 0.01 is sufficient.

https://doi.org/10.5194/wes-2023-2
Preprint. Discussion started: 17 February 2023

eawe european academy of wind energy
Open Access WIND ENERGY SCIENCE DISCUSSIONS

3 Results of Computational Experiments

In this section we use representative examples to demonstrate the potential of dynamic wind farm control by axial induction. The computational experiments are divided into two test series, each containing some cases.

As mentioned before, all cases have in common the wind turbine number of $n_{\mathrm{WT}} = 2$ and the turbulence intensity of $I = 0.01$, see Sect. 2.1. Further, the number of intermediate knots (for the cubic spline interpolation) is $n_{\mathrm{ctrl}} = 9$, see Sect. 2.4.2. The other parameters depend on the test series or the contained cases: This concerns the average wind speed U_{ave}, see Sect. 2.1, the fatigue reference value $u_{\mathrm{f,v}}$ for both wind turbines, see Sect. 2.2, the tower activity weight ω_{T} and the pitch activity weight ω_{P}, see Eq. (3).

Experimental Design. We want to explore several effects: We are interested in the effect of power reference optimization itself, i.e., in comparison to baseline (greedy) in terms of the three performance indicators (power, tower activity and pitch activity). We will consider the effect of the tower activity weight and the pitch activity weight comparing optimization results to each other. Further, we are interested in the effect of fatigue reduction, i.e., active tower damping, comparing optimization to baseline. We will also study the effects of these configuration combinations (comparing optimization results to each other). Of course, we have to consider different wind gusts for a meaningful result. All in all, we make two test series.

The considered NREL 5-MW wind turbines have a cut-in, rated and cut-out wind speed of $3\,\mathrm{m\,s^{-1}}$, $11.4\,\mathrm{m\,s^{-1}}$ and $25\,\mathrm{m\,s^{-1}}$, see (Jonkman et al., 2009, Table 1-1). Of course, it is interesting to investigate a wind gust that exceeds the rated speed. In addition, we consider one below and one above. Finally, we choose 6–7 $\mathrm{m\,s^{-1}}$, 11–12 $\mathrm{m\,s^{-1}}$ and 12–13 $\mathrm{m\,s^{-1}}$ as representative examples.

Series 1. In series 1, we consider three different wind gusts: 6–7 $\mathrm{m\,s^{-1}}$, 11–12 $\mathrm{m\,s^{-1}}$ and 12–13 $\mathrm{m\,s^{-1}}$, i.e., a wind speed change of $1\,\mathrm{m\,s^{-1}}$. For every wind gust, we consider four different control configurations: without/with fatigue reduction, i.e., fatigue reference value $u_{\mathrm{f,v}} = 0$ or 1, and without/with tower activity weight, i.e., $\omega_{\mathrm{T}} = 0$ or 100.

The different cases are numbered in ascending order, see Table A1. In total series 1 comprises 12 cases. All experiments of series 1 are without pitch activity weight, i.e., $\omega_{\mathrm{P}} = 0$.

Series 2. In comparison to series 1, we use the pitch activity weight in series 2, i.e., we set $\omega_{\mathrm{P}} = 10$, to investigate its effect. We only consider a wind speed of 11–12 $\mathrm{m\,s^{-1}}$. Similar to series 1, we simulate control configurations without/with fatigue reduction and without/with tower activity weight (using the same weight value ω_{T} as in series 1). The experiments are numbered, see Table A2.

Choice of Weights. We have chosen both weights, i.e., power activity weight $\omega_{\mathrm{T}} = 0$ or 100 and pitch activity weight $\omega_{\mathrm{P}} = 0$ or 10, such that they have a significant effect.[11]

[11] For an impression of the effect's significance, we look at the data in advance: with the results of the baseline of series 1 case 5 (i.e., a power of 6.291 MW, a tower activity of 0.012 and a pitch activity of 0.077) this would result in proportions of 19% (for tower activity with weight) and 12% (for pitch activity with weight) compared to power.

https://doi.org/10.5194/wes-2023-2
Preprint. Discussion started: 17 February 2023

eawe european academy of wind energy
Open Access WIND ENERGY SCIENCE DISCUSSIONS

Table 2. Time intervals (see Sect. 2.1 for a definition), iterations and run time of some cases of test series 1: The cases 1, 5 and 9 belong to the average wind speeds 6, 7, 6–7 $\mathrm{m\,s^{-1}}$ (case 1), 11, 12, 11–12 $\mathrm{m\,s^{-1}}$ (case 5), and 12, 13, 12–13 $\mathrm{m\,s^{-1}}$ (case 9). Remember that the dynamic control time interval is $[t_{\mathrm{c}_1}, t_{\mathrm{c}_2}]$, that t_{s_2} is the end of the simulation time interval $[t_{\mathrm{s}_1}, t_{\mathrm{s}_2}]$ (with $t_{\mathrm{s}_1} = 0$), and that $[t_{\mathrm{o}_1}, t_{\mathrm{o}_2}]$ is the observation time interval. The iterations of fmincon are given for the scenarios 1, 2 and 3, i.e., low wind speed, high wind speed and wind gust. The run time is the total one for scenarios 1, 2 and 3.

Case (No.)	$[t_{\mathrm{c}_1}, t_{\mathrm{c}_2}]$ in s	t_{s_2} in s	$[t_{\mathrm{o}_1}, t_{\mathrm{o}_2}]$ in s	Iterations (scenarios 1, 2, 3)	Run time in min
1	[353, 509]	695	[312, 695]	7, 6, 3	91
5	[186, 268]	380	[164, 380]	7, 1, 2	44
9	[166, 238]	341	[146, 341]	1, 1, 1	26

Structure. The results, evaluations and summary of series 1 and 2 are in the tables in App. A. The corresponding figures of the optimization results in the scenario with wind gust are in App. B. We explain the tables and figures in Sect. 3.1 and discuss the effect of control inputs, weights and wind conditions in Sect. 3.2. Thereby we repeat and add some figures.

Computational Set-Up. All computations were carried out on a workstation with an Intel(R) Core(TM) i7-6700 CPU with 3.40 GHz and 32 GByte RAM using MATLAB in version R2019b. The run time of one simulation mainly depends on the simulation time interval (for the same wind farm layout), which depends on the wind speed. Of course, the total run time also depends on the number of iterations of the optimization method. Some time intervals, number of iterations and run times are given in Table 2.

3.1 Explanation of Tables and Figures

As already mentioned, the tables are in App. A. They are divided into results, see Tables A1 and A2, evaluations, see Tables A3–A5, and a summary (of these evaluations), see Table A6. The corresponding figures are in App. B. For example, series 1 case 5 is in Table A1 and Fig. B2(a) (also in Fig. 5(b) for discussion). We describe the content of them using examples to become familiar with the tables and figures. However, an interpretation of the effects will follow in the next section.

Results Tables. We choose series 1 case 5 as leading example, see Table A1. We read from the results table that this case includes scenarios with a low wind speed (scenario 1) of $U_\ell = 11\,\mathrm{m\,s^{-1}}$, a high wind speed (scenario 2) of $U_\mathrm{h} = 12\,\mathrm{m\,s^{-1}}$ and a wind gust (scenario 3) with wind speed U_ave of 11–12 $\mathrm{m\,s^{-1}}$. Note that all wind gust rows are highlighted by a bottom border (in Tables A1 and A2). Further, the fatigue reference values of both wind turbines are set to $u_{\mathrm{f,v}} = 0$, i.e., without fatigue reduction. The tower activity weight is set to $\omega_\mathrm{T} = 0$. We remember that the pitch activity weight is $\omega_\mathrm{P} = 0$ for series 1.

The output is divided into *baseline* (i.e., greedy control) and *optimization* (with the method described in Sect. 2.4) results, each consisting of the three performance indicators power P, tower activity a_T and pitch activity a_P, see Sect. 2.2. (Remember

https://doi.org/10.5194/wes-2023-2
Preprint. Discussion started: 17 February 2023

eawe european academy of wind energy
Open Access WIND ENERGY SCIENCE DISCUSSIONS

that theses are the individual values of the objective function Eq. (3) and the units of tower activity and pitch activity have no physical meaning.) In particular, for the baseline we denote them by P_b, $a_{\mathrm{T,b}}$, $a_{\mathrm{P,b}}$ and for the optimization by P_o, $a_{\mathrm{T,o}}$, $a_{\mathrm{P,o}}$.

The evaluation ratios in the results tables, see Tables A1 and A2, always compare the optimization results to the *corresponding baseline*, i.e., the baseline in the same line. However, in the evaluation tables, see Tables A3–A5, the evaluation ratios compare the optimization results to the associated *raw baseline*, i.e., always the corresponding baseline without fatigue reduction. In Table A1 for average wind speeds of 11, 12 and 11–12 $\mathrm{m\,s^{-1}}$ these are the baselines of cases 5 and 6. We only highlight one representative of the associated raw baseline outputs in the results tables with a frame, see Tables A1 and A2. We make it clear in the column heading what quantity we are referring to.

In the results tables we want to see the change of the optimization compared to the corresponding baseline, i.e., in the same line. Therefore, we compute the ratios[12] of the optimization in comparison to the corresponding baseline in percent, i.e.,

$$r_\mathrm{P} = 100\,\frac{P_\mathrm{o}}{P_\mathrm{b}} - 100, \quad r_{\mathrm{a_T}} = 100\,\frac{a_{\mathrm{T,o}}}{a_{\mathrm{T,b}}} - 100, \quad r_{\mathrm{a_P}} = 100\,\frac{a_{\mathrm{P,o}}}{a_{\mathrm{P,b}}} - 100.$$

We will speak abbreviated from the ratio to the corresponding baseline. Note that we write "–" in the table if the computation of the ratio would lead into a division by 0.

In the example of series 1 case 5 with wind gust (11–12 $\mathrm{m\,s^{-1}}$), see Table A1, the power increases 5.1%, the tower activity decreases 2.4% and the pitch activity decreases 7.3% (in comparison to baseline). In that case, the optimization has the desired effect on all three performance indicators.

Further, remember that tower activity weight and pitch activity weight influence the optimization result but not the baseline result. Therefore, the baseline results of series 1 cases 5 and 6 are the same.

Evaluation Tables. To work out effects, we compare results among each other in the evaluation tables. For this we make two comparisons.

First, in Tables A3 and A4 the optimization results are compared to the associated *raw baseline*, i.e., always the corresponding baseline without fatigue reduction. (As described above, one representative is highlighted with a frame.) This means, we compute the ratio for the power as $100\,(P_\mathrm{o}/P_{\mathrm{b,r}}) - 100$ and the ratios for the activities a_T and a_P analog. (To make clear, that we include optimization of the power reference value, we use the column header $u_{\mathrm{p,v}}$ *opt.* and set it to 1.)

Second, in Table A5 the results of baseline (not optimization) with fatigue reduction are compared with baseline without fatigue reduction (which is the associated raw baseline). Therefore, we focus on cases 3, 7 and 11 (and $u_{\mathrm{p,v}}$ *opt.* is 0). This means, we compute the ratio for the power as $100\,(P_\mathrm{b}/P_{\mathrm{b,r}}) - 100$ and the ratios for the activities a_T and a_P analog. We only consider comparisons in scenario 3 (i.e., wind gust scenario).

Example to the Evaluation Tables. For example, we are interested in the effect of the tower activity weight ω_T for the wind speed of 11–12 $\mathrm{m\,s^{-1}}$. In Table A3 we have series 1 case 5 ($\omega_\mathrm{T} = 0$) and 6 ($\omega_\mathrm{T} = 100$) in comparison to the raw baseline. The changes of power, tower activity and pitch activity are 5.1%, -2.4%, -7.3% (case 5) and 7.9%, -18.7%, 37.3% (case 6).

[12] It is more natural to use the transformation $r_\mathrm{P} = 100\,(P_\mathrm{o} - P_\mathrm{b})/P_\mathrm{b}$, but the used representation saves symbols.

https://doi.org/10.5194/wes-2023-2
Preprint. Discussion started: 17 February 2023

eawe european academy of wind energy
Open Access WIND ENERGY SCIENCE DISCUSSIONS

This means, that the (used) tower activity weight increases the power (7.9% instead of 5.1%), decreases the tower activity but increases the pitch activity.

In cases 5 and 6 of series 1, the ratios in the results table, see Table A1, are the same as in the evaluation table, see Table A3, as the baseline in the same line and the raw baseline coincide. This is not the case if the fatigue reference is set to 1 as, e.g., in series 1 case 7. In that example, the changes of power, tower activity and pitch activity are 5.1%, -3.8%, 0.7% in comparison to the baseline in the same line (i.e., with fatigue reduction), see Table A1, but 5.1%, -59.3%, 96.6% in comparison to the raw baseline (i.e., the corresponding baseline without fatigue reduction), see Table A3.

Summary Table. The results for the wind gusts (scenario 3) of all evaluation tables are summarized in Table A6. (Remember that ratio has different meanings: It compares optimization with associated raw baseline if the quantity reference is power. It compares baseline result with associated raw baseline if the quantity reference is fatigue.) For example, we find the evaluation of series 1 cases 1, 5 and 9 in the first row. These are the corresponding cases to wind gusts with average wind speed of 6–7 $\mathrm{m\,s^{-1}}$, 11–12 $\mathrm{m\,s^{-1}}$ and 12–13 $\mathrm{m\,s^{-1}}$. Essentially, we will use this table to discuss the results. Of course, sometimes it is useful to look at the details in results tables or evaluation tables.

Figures. As already mentioned, figures of all cases are in App. B. This is restricted to optimization (not baseline) results of scenario 3, i.e., the wind gust scenario. In the discussion of the results we additionally show some baseline results for comparison and we repeat interesting parts of the appendix to draw attention. In all figures we give the time in the unit s and focus on the observation time interval. Further, the quantities for the upstream wind turbine are depicted in blue and for the downstream one in red. The figures can contain the following quantities:

- powerRefCtrl (without unit) is the *power reference value* $u_{\mathrm{p,v}} \in [0.5, 1]$, which is an input of the local wind turbine controller. It is our main control input for the wind farm control, see Sect. 2.2. (Remember that it is fixed to 1 for the downstream wind turbine.)
- GenTq (in $\mathrm{N\,m}$) is the *generator torque*. It is controlled by the local wind turbine controller.
- BldPitch1 (in $^\circ$) is the *blade pitch angle* of the first rotor blade. As we do not use individual blade pitch control, the angle is the same for the other blades. The angle is controlled by the local wind turbine controller.
- GenSpeed (in rpm) is the *generator speed*, which is an output quantity.
- GenPwr (in W) is the generator *power*, whose average (in MW) is our main performance indicator.
- Wind1VelX (in $\mathrm{m\,s^{-1}}$) is the hub-height *wind speed* (in x direction, i.e., here in the direction of the straight line drawn by the wind turbines).
- NclMuTVxs (in $\mathrm{m\,s^{-1}}$) is the *nacelle fore-aft velocity* (in x direction), which is an output quantity.

https://doi.org/10.5194/wes-2023-2
Preprint. Discussion started: 17 February 2023

eawe european academy of wind energy
Open Access WIND ENERGY SCIENCE DISCUSSIONS

We discuss Fig. 5, which shows series 1 case 5, in the next section. At this point, we only point out that both power references are 1 for baseline, see Fig. 5(a), and we remember that the limit of the power reference is 1 and that it is always set to 1 for the downstream wind turbine, see Fig. 5(b).

3.2 Effects of Control Inputs, Weights and Wind Conditions

We discuss the effects on our performance indicators, i.e., power, tower activity and pitch activity, with respect to the control inputs, i.e., optimal power reference (for the upstream wind turbine) and without/with fatigue reduction (for both wind turbines). In the case of power reference this is done in dependence of the used weights on tower activity and pitch activity. Further, the wind conditions, i.e., wind speeds, play a role.

3.2.1 Effect of Optimization

The evaluation in Table A1 (series 1, i.e., pitch activity weight $\omega_{\mathrm{P}} = 0$) and Table A2 (series 2, i.e., pitch activity weight $\omega_{\mathrm{P}} = 10$) compares respectively the optimization result with the baseline simulation in the same line (of the table). Therefore, it shows the effect of the optimization itself.

Power. In the case of series 1 the power increases or is unchanged. Most of the unchanged cases can be explained with the wind speed: If the wind speed is $12\,\mathrm{m\,s^{-1}}$ or higher (cases 9 to 12), baseline (greedy) was already the best choice. The only exception is case 4 with a wind speed of 6–7 $\mathrm{m\,s^{-1}}$. The power remains unchanged. In that case the fatigue reduction already reduces the tower activity in the baseline; in addition, we weight the tower activity in the optimization; probably, this prevents an increase in power; however, it is also possible to have reached a local minimum.

In the case of series 2 the effect of optimization is different. The chosen pitch activity weight results in the case of constant wind speeds sometimes in an increase and sometimes in a decrease of power. The limitation of the pitch activity prevents higher power in many cases. However, in the scenarios with the wind gust, the power always increases.

All in all, the power increases between 2% and 8% in the scenarios with wind gust (in series 1 and 2). The only exception is the discussed case 4 with 6–7 $\mathrm{m\,s^{-1}}$ of series 1.

Tower Activity. The most interesting cases in series 1 are the ones, that have a wind gust: in the cases of 6–7 $\mathrm{m\,s^{-1}}$ the optimization can not contribute to reduction of tower activity, although we weight it in the cases 2 and 4. However, we remember that the increase in power and the decrease in tower activity are opposed aims.

This balancing act succeeds in the case of 11–12 $\mathrm{m\,s^{-1}}$ in series 1 as well as series 2: optimization itself increases the power and reduces the tower activity.

As already mentioned, if the wind speed is $12\,\mathrm{m\,s^{-1}}$ or higher (series 1 cases 9 to 12), baseline (greedy) was already the best choice; so, there is no effect of optimization on the tower activity.

Pitch Activity. In test series 1 we do not penalize the pitch activity. It is not surprising that the pitch activity sometimes decreases and sometimes increases (compared to baseline in the same line).

https://doi.org/10.5194/wes-2023-2
Preprint. Discussion started: 17 February 2023

eawe european academy of wind energy
Open Access WIND ENERGY SCIENCE DISCUSSIONS

In test series 2 the weight $\omega_{\mathrm{P}} = 10$ takes an effect. The pitch activity is significantly reduced in all cases.

Example in Table. For example, the effect of optimized control in comparison to baseline control is in ratios of power, tower activity and pitch activity: $+5.1\%$, -2.4%, -7.3%, see case 5 of series 1 in Table A1.

Summary Table. Remember that the summary table, see Table A6, contains the ratios to the raw baseline instead of the baseline in the same line. Therefore, it provides a good overview, but it shows not only the effect of the optimization.

Example Figure. The effect of optimization describes the effect of an optimal power reference for the upstream wind turbine. We briefly consider Fig. 5 comparing the baseline result in Fig. 5(a) and the optimization result in Fig. 5(b). The corresponding dataset is series 1 case 5, i.e., a wind speed of 11–12 $\mathrm{m\,s^{-1}}$ without fatigue reduction, without tower activity weight and without pitch activity weight.

As already mentioned, we usually only present the optimization result as in Fig. B2(a); however, the difference should become clear once.

Of course, the power reference values of both turbines are 1 for baseline. In optimization the controller ensures a relatively straight transition from the low to the high steady state power reference value. Further, we consider the limit at a power reference of 1.

For both (baseline and optimization), the wind gust approaches the upstream wind turbine at about $t = 220\,\mathrm{s}$. We consider a comparable control reaction to turbulence: before the wind gust only (in baseline) or mainly (in optimization) due to generator torque; afterwards mainly due to blade pitch angle and little due to generator torque. The reason is the rated wind speed of 11.4 $\mathrm{m\,s^{-1}}$ for the considered NREL 5-MW wind turbines, see (Jonkman et al., 2009, Table 1-1). Therefore, the wind speed of 11–12 $\mathrm{m\,s^{-1}}$ is particularly interesting. For both, we consider an abrupt increase of the generator torque when the wind gust arrives.

In contrast, the generator speed has no abrupt changes. However, the generator power follows the generator torque. Of course, at the upstream wind turbine the wind gust arrives at once. The later arrive at the downstream wind turbine is staircase-like as the wind speed is influenced by the power reference of the upstream wind turbine. The nacelle fore-aft velocity gives an impression of the tower oscillation. Essentially, they appear in the context of wind changes (and finally show up in the tower activity).[13]

3.2.2 Effect of Wind Speed

As already mentioned, if the wind speed is 12 $\mathrm{m\,s^{-1}}$ or higher (cases 9 to 12), baseline (greedy) was already the best choice, see Table A1. For a direct comparison to the already considered case of 11–12 $\mathrm{m\,s^{-1}}$ (series 1 case 5) in Fig. 5(b), we show the corresponding case of 12–13 $\mathrm{m\,s^{-1}}$ (series 1 case 9) in Fig. 6(b) and the case of 6–7 $\mathrm{m\,s^{-1}}$ (series 1 case 1) in Fig. 6(a).

[13] This observation suggests to substitute the tower activity with the wind speed changes (e.g., for real-time online optimization). However, the use of this observation is not part of this paper.

https://doi.org/10.5194/wes-2023-2
Preprint. Discussion started: 17 February 2023

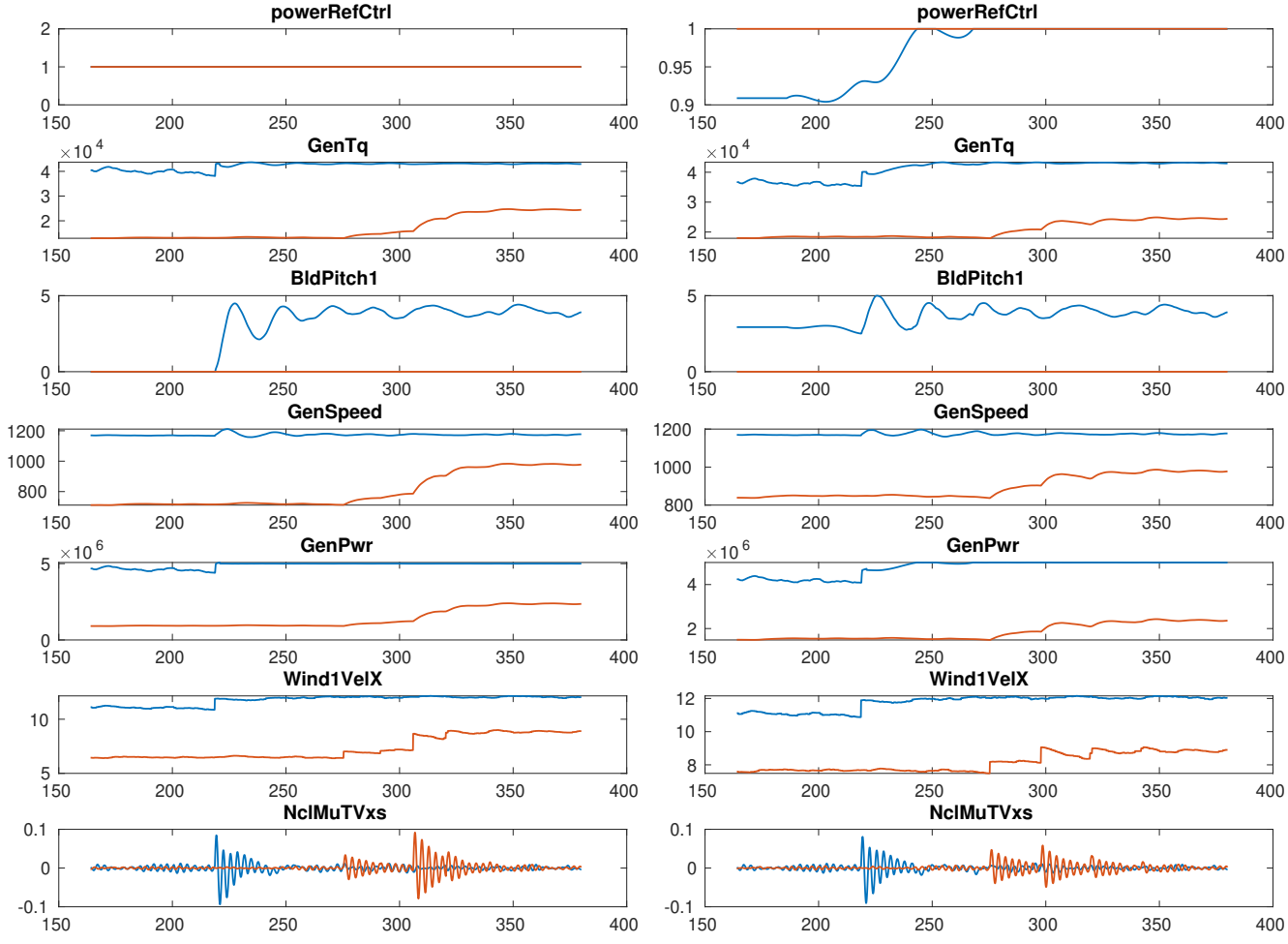

(a) Test series 1 case 5 baseline (greedy).

(b) Test series 1 case 5 optimization.

Figure 5. Effect of optimization (test series 1 case 5). All quantities are depicted over the time in s, which we restrict to the observation time interval. The quantities for the upstream wind turbine are depicted in blue and for the downstream one in red. The wind gust increases the average wind speed (11–12 $\mathrm{m\,s^{-1}}$). (a) Baseline simulation, i.e., no individual power reduction (both wind turbines run greedy with power reference values of $u_{\mathrm{p,v}} = 1$). (a) Optimization result, i.e., control of power reference value $u_{\mathrm{p,v}}$ of upstream wind turbine (and $u_{\mathrm{p,v}} = 1$ for the downstream one). Remember that series 1 does not use pitch activity weight, i.e., $\omega_{\mathrm{P}} = 0$. In particular, case 5 is without fatigue reduction, i.e., $u_{\mathrm{f,v}} = 0$ for both wind turbines, and without tower activity weight, i.e., $\omega_{\mathrm{T}} = 0$.

Both cases are not as instructive as 11–12 $\mathrm{m\,s^{-1}}$. The summary table, see Table A6, offers a similar impression. Usually, 6–7 $\mathrm{m\,s^{-1}}$ and 12–13 $\mathrm{m\,s^{-1}}$ have either no effect or a similar effect as 11–12 $\mathrm{m\,s^{-1}}$. (There are two exceptions for 6–7 $\mathrm{m\,s^{-1}}$: without fatigue reduction, without/with tower activity weight, without pitch activity weight.)

Therefore, we will mainly focus on 11–12 $\mathrm{m\,s^{-1}}$ in the following discussion.

https://doi.org/10.5194/wes-2023-2
Preprint. Discussion started: 17 February 2023

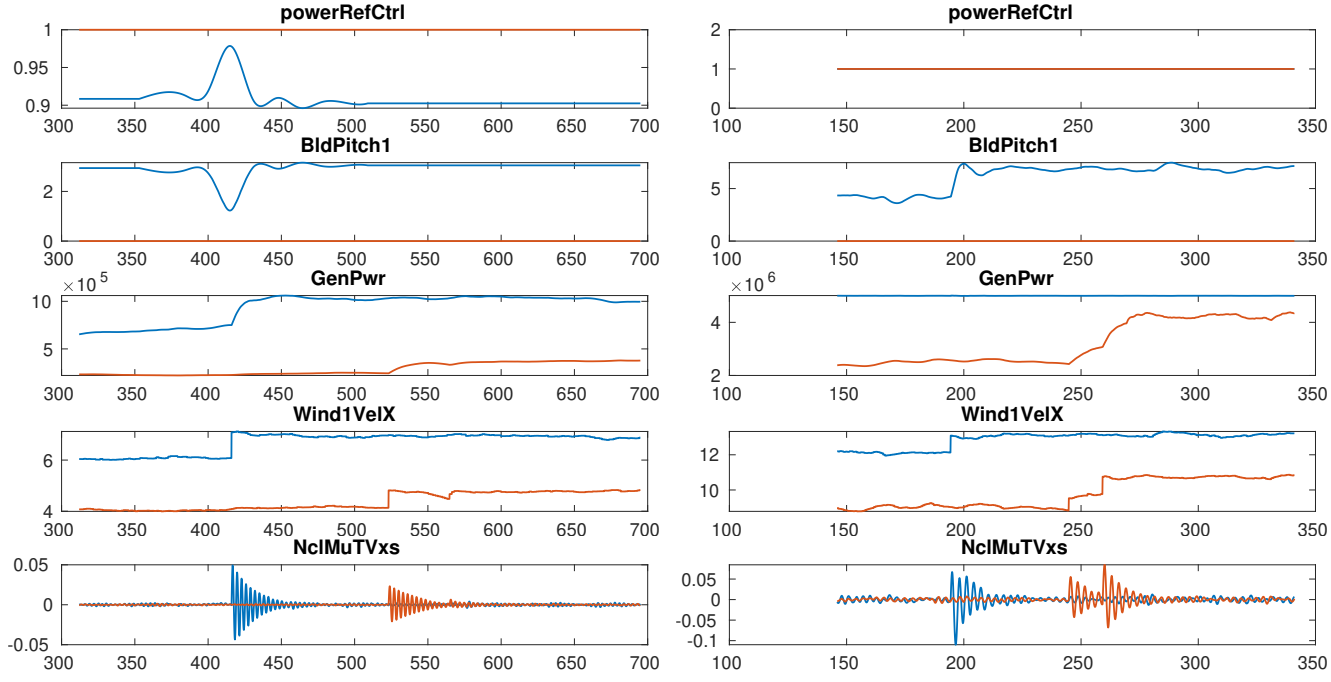

(a) Test series 1 case 1 optimization.

(b) Test series 1 case 9 optimization.

Figure 6. Effect of wind speed. Test series 1 cases 1 (6–7 $\mathrm{m\,s^{-1}}$) and 9 (12–13 $\mathrm{m\,s^{-1}}$) (both with fatigue reference value $u_{\mathrm{f,v}} = 0$, tower activity weight $\omega_{\mathrm{T}} = 0$, and pitch activity weight $\omega_{\mathrm{P}} = 0$). For the corresponding case 5 (11–12 $\mathrm{m\,s^{-1}}$), see Fig. 5(b).

3.2.3 Effect of Weight on Tower Activity and Pitch Activity

For the effect of weight on tower activity and pitch activity, we compare optimization results among each other. Thereby, the comparative value is the raw baseline, i.e., the corresponding baseline without fatigue reduction.

As already mentioned, the power activity weight is $\omega_{\mathrm{T}} = 0$ or $\omega_{\mathrm{T}} = 100$ and the pitch activity weight is $\omega_{\mathrm{P}} = 0$ or $\omega_{\mathrm{P}} = 10$ to have a significant effect.

For comparison, we focus on the wind speed of 11–12 $\mathrm{m\,s^{-1}}$ without fatigue reduction, i.e., series 1 cases 5 and 6 as well as series 2 cases 1 and 2, that are depicted in Fig. 7. For the changes we also refer to Table A6.

Tower Activity Weight. First, we compare the optimization result with tower activity weight of $\omega_{\mathrm{T}} = 100$ in Fig. 7(b) (series 1 case 6) to the result with $\omega_{\mathrm{T}} = 0$ in Fig. 7(a) (series 1 case 5). The velocity of the nacelle, NclMuTVxs, is significantly reduced for the downstream wind turbine, which results in a reduced tower activity (-18.7% instead of -2.4% compared to raw baseline). An increase of the pitch activity was expected (37.3% instead of -7.3%). The increase of power (7.9% instead of 5.1%) may come as a surprise, but as we can not expect a global solution, the tower activity weight seems to stabilize the solution. Note that the main effect of tower activity is at the downstream wind turbine (in comparison to raw baseline in

https://doi.org/10.5194/wes-2023-2
Preprint. Discussion started: 17 February 2023

brackets): upstream wind turbine 0.0065 (0.0059), downstream wind turbine 0.0034 (0.0064). Finally, the control of the power reference of an upstream wind turbine is an effective method to increase overall power and decrease tower activity.

Pitch Activity Weight. Second, we compare the optimization result with pitch activity weight of $\omega_{\mathrm{P}} = 10$ in Fig. 7(c) (series 2 case 1) to $\omega_{\mathrm{P}} = 0$ in Fig. 7(a) (series 1 case 5). The pitch activity is reduced within the scope of possibilities, i.e., the power reference value only changes from optimal value for average low wind speed to optimal value for high wind speed. This leads to little influence on the blade pitch angle. However, the blade pitch angle has changes due to the internal wind turbine controller. Power, tower activity and pitch activity are (compared to raw baseline) of 1.7%, -17.1%, -39.0% (instead of 5.1%, -2.4%, -7.3%). The power is higher than in the baseline result but lower as in the case of optimization only in regard to power. Note that the main effect of tower activity is again at the downstream wind turbine (in comparison to $\omega_{\mathrm{P}} = 0$ in brackets): upstream wind turbine 0.0057 (0.0059), downstream wind turbine 0.0045 (0.0060).[14] Finally, the method is effective to decrease the pitch activity. At the same time, the tower activity is reduced.

Tower and Pitch Activity Weight. Third, we compare the combination a tower activity weight of $\omega_{\mathrm{T}} = 100$ and a pitch activity weight of $\omega_{\mathrm{P}} = 10$ in Fig. 7(d) (series 2 case 2) to the other combinations. Power, tower activity and pitch activity are (compared to raw baseline) of 5.6%, -17.9%, -22.0%. So, the power increase (5.6%) is not as high as in the best case (7.9% with $\omega_{\mathrm{T}} = 100$ and $\omega_{\mathrm{P}} = 0$), but much higher than in the worst case (1.7% with $\omega_{\mathrm{T}} = 0$ and $\omega_{\mathrm{P}} = 10$). The tower activity decrease (-17.9%) is slightly lower than the best[15] (-18.7% with $\omega_{\mathrm{T}} = 100$ and $\omega_{\mathrm{P}} = 0$). The pitch activity decrease (-22.0%) is lower than in the best case (-39.0% with $\omega_{\mathrm{T}} = 0$ and $\omega_{\mathrm{P}} = 10$) but much better than the other cases (-7.3% with $\omega_{\mathrm{T}} = 0$ and $\omega_{\mathrm{P}} = 0$ and 37.3% with $\omega_{\mathrm{T}} = 100$ and $\omega_{\mathrm{P}} = 0$).

Summary. All in all, we recommend to weight the tower activity as it first, significantly decreases the tower activity and second, not necessarily counteracts the conflicting objective to power increase. If a decrease of the pitch activity is important, we recommend to weight the pitch activity additionally as it first, significantly decreases the pitch activity and second, has a moderate influence on the conflicting objective of power increase. However, in practice, a low tower activity is more important than a low pitch activity.

3.2.4 Effect of Fatigue Reduction

For the effect of fatigue reduction, we compare first, baseline results among each other and second, optimization results among each other. Again, we focus on the results with a wind speed of 11–12 $\mathrm{m\,s^{-1}}$ as the results of 6–7 $\mathrm{m\,s^{-1}}$ and 12–13 $\mathrm{m\,s^{-1}}$ are very similar. As already mentioned, we compute either without ($u_{\mathrm{f,v}} = 0$) or with ($u_{\mathrm{f,v}} = 1$) fatigue reduction.

[14] The raw data of power are at upstream wind turbine 4.4093 MW (4.7655 MW), at downstream 1.991 MW (1.8479 MW) and of pitch activity at upstream 0.0467 (0.0709), downstream 0 (0) (as the power reference value of the downstream wind turbine is fixed).

[15] At this point, we do not consider the results with fatigue reduction.

https://doi.org/10.5194/wes-2023-2
Preprint. Discussion started: 17 February 2023

eawe european academy of wind energy
Open Access WIND ENERGY SCIENCE DISCUSSIONS

Fatigue Reduction in Baseline. First, the only effect of fatigue reduction (without optimization) is considered. Therefore, we compare the baseline with fatigue reduction with the corresponding baseline without fatigue reduction. These comparisons are summarized in Table A5. For the wind gust, the results can also be found in Table A6.

For the wind speed of 11–12 $\mathrm{m\,s^{-1}}$, the baseline results without/with fatigue reduction are in Fig. 8. The corresponding ratios of power, tower activity and pitch activity are 0.0%, -57.7% and 95.3%. So, the power is the same.[16] For the significantly reduced tower activity, we have to accept a high pitch activity.[17] Note that the (used) fatigue reduction has a significant influence on both wind turbines regarding the tower activity. In comparison, we remember that the main effect of the (used) tower activity weight was only at the downstream wind turbine. Furthermore, the effect of the fatigue reduction on tower activity is stronger than the effect of the considered tower activity weight.

Fatigue Reduction in Optimization. Second, we consider the effect of fatigue reduction with optimization of the power reference value. In Fig. 9 we have the optimization results for 11–12 $\mathrm{m\,s^{-1}}$ with fatigue reduction and without pitch activity weight for both cases without/with tower activity weight, i.e., we can compare Fig. 9(a) (series 1 case 7: $u_{\mathrm{f,v}} = 1$, $\omega_{\mathrm{T}} = 0$) with Fig. 7(a) (series 1 case 5: $u_{\mathrm{f,v}} = 1$, $\omega_{\mathrm{T}} = 0$) and we can compare Fig. 9(b) (series 1 case 8: $u_{\mathrm{f,v}} = 1$, $\omega_{\mathrm{T}} = 100$) with Fig. 7(b) (series 1 case 6: $u_{\mathrm{f,v}} = 1$, $\omega_{\mathrm{T}} = 100$).

The ratios with fatigue reduction are in the case without tower activity weight (series 1 case 7): power 5.1% (instead of 5.1% in series 1 case 5), tower activity -59.3% (instead of -2.4%) and pitch activity 96.6% (instead of -7.3%). So, we observe an effect as in the baseline case: The power is the same. For the significantly reduced tower activity, we have to accept a high pitch activity.

The ratios with fatigue reduction are in the case with tower activity weight (series 1 case 8): power 5.2% (instead of 7.9% in series 1 case 6), tower activity -63.4% (instead of -18.7%), pitch activity 74.2% (instead of 37.3%).[18] In comparison to the effect in the baseline case, the same power is not reached.

Finally, the combination of fatigue reduction and tower activity weight is useful to decrease the tower activity: ratios of tower activities are -63.4% (with tower activity weight) and -59.3% (without).

The highest decrease of tower activity ratio is reached with fatigue reduction, tower activity weight and pitch activity weight: -74.8%. The pitch activity ratio is moderate (8.6%), but the power ratio is only 4.0% in that case.

Summary. Indeed, the (used) fatigue reduction decreases the tower activity significantly. In return, we have to accept a very high pitch activity (if we do not activate the pitch activity weight). However, the (used) fatigue reduction is not necessarily adverse to the power.

[16] Furthermore, there are also no significant changes in the individual wind turbines. The raw data for the power of the wind turbines are with fatigue reduction (series 1 case 7) in comparison without fatigue reduction (series 1 case 5): 4.9028 instead of 4.9029 for the upstream wind turbine and 1.3888 instead of 1.3884 for the downstream wind turbine.

[17] Raw data of tower activity: 0.0030 instead of 0.0059 for upstream and 0.0022 instead of 0.0063 for downstream. Raw data of pitch activity: 0.0968 instead of 0.0765 and 0.0526 instead of 0.0000.

[18] Furthermore, if we compare the pitch activity of series 1 case 8 to 7, we observe a decrease of pitch activity for both wind turbines. The raw data for the pitch activity of the wind turbines are with tower activity weight (series 1 case 8) in comparison without tower activity weight (series 1 case 7): 0.0891 (instead of 0.0982) for the upstream wind turbine and 0.0441 (instead of 0.0522) for the downstream one.

https://doi.org/10.5194/wes-2023-2
Preprint. Discussion started: 17 February 2023

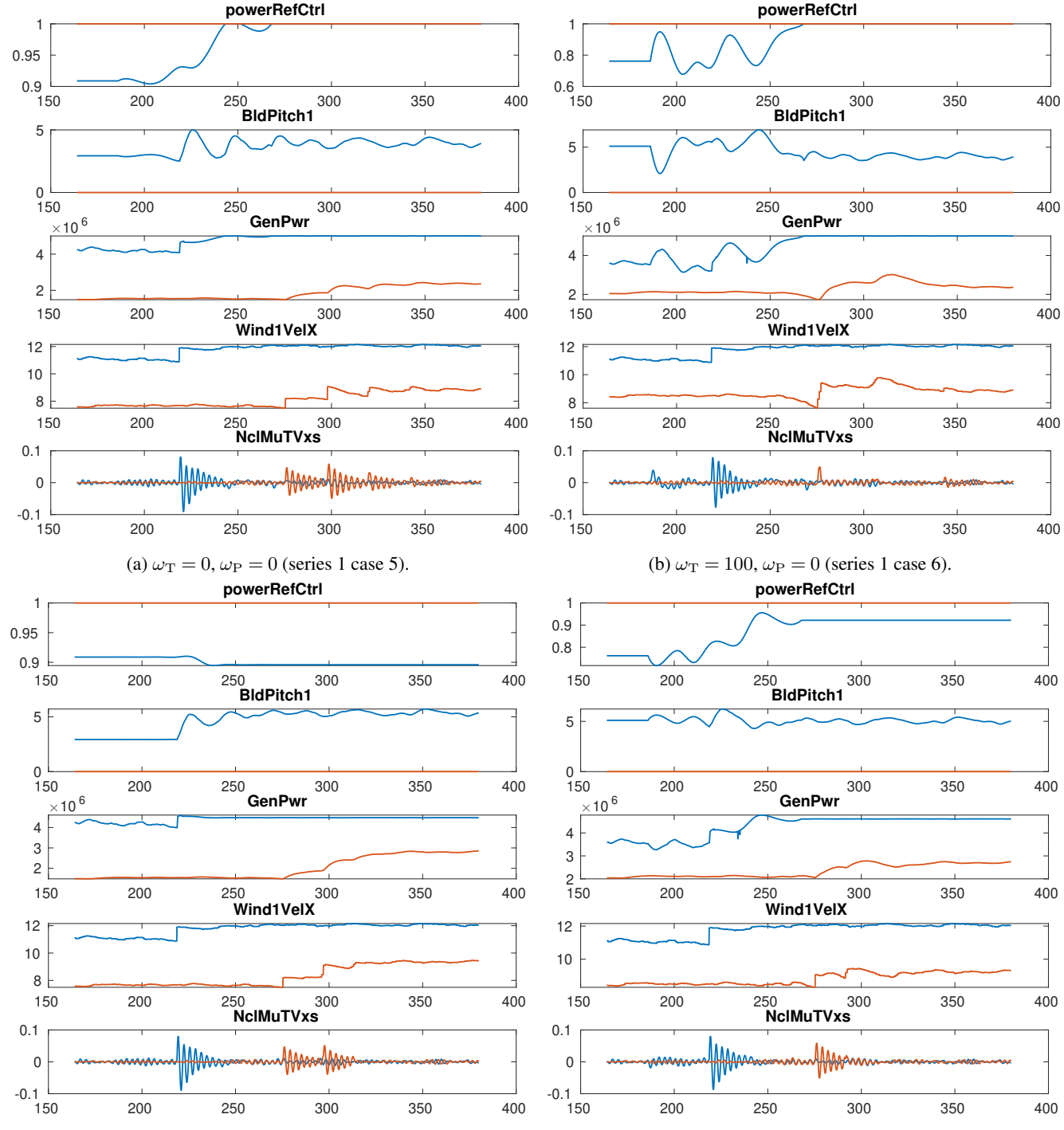

(a) $\omega_T = 0$, $\omega_P = 0$ (series 1 case 5).

(b) $\omega_T = 100$, $\omega_P = 0$ (series 1 case 6).

(c) $\omega_T = 0$, $\omega_P = 10$ (series 2 case 1).

(d) $\omega_T = 100$, $\omega_P = 10$ (series 2 case 2).

Figure 7. Effect of tower activity weight and pitch activity weight (without fatigue reduction). (We repeat series 1 case 5 for sake of easier comparison.) Note that (c) is a rare example of an optimal lower power reference value at high wind speed than at low wind speed.

https://doi.org/10.5194/wes-2023-2
Preprint. Discussion started: 17 February 2023

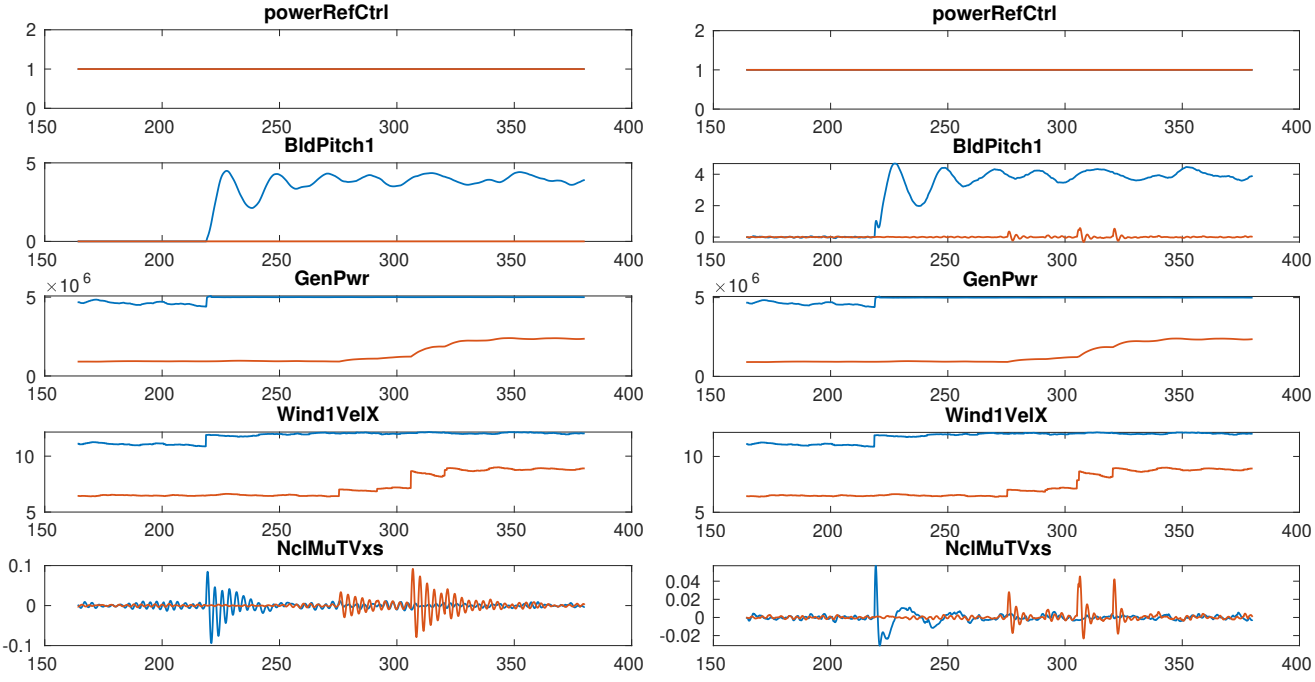

(a) $u_{\mathrm{f,v}} = 0$ (series 1 case 5). (b) $u_{\mathrm{f,v}} = 1$ (series 1 case 7).

Figure 8. Effect of fatigue reduction in baseline result (test series 1 cases 5 and 7).

4 Conclusions

In this paper we investigated the potential of axial-induction-based dynamic control in the case of a wind gust to increase the power and decrease the load. To do this proof of concept, we used error free simulation data and did not pay particular attention to the run time. A wind gust requires a dynamic control reaction and the consideration of the time delay with which downstream turbines are affected. On the other hand, this requirement is a chance: Besides the expected increase in total power, we point out the option to reduce the tower load of downstream wind turbines by dynamic axial-induction-based control of an upstream turbine. Further, we can take care of the pitch activity. We both realized by taking into account the tower activity and the pitch activity in the objective function (with appropriate weighting). To the best of our knowledge, we are the first reducing the tower load by dynamically controlling an upstream wind turbine. As we know the wind speed a priori, it is an offline optimization. However, this provides an impression of the potential of real-time online optimization.

Code and data availability. For simulation we use the MATLAB software package WinFaST as already mentioned in Sect. 1. It is unpublished as it is an internal company software package. However, as described in Sect. 2.1 it is essentially based on known methods: the dynamic wake model relies on FLORIDyn, see Gebraad and van Wingerden (2014), and the controller relies on Jonkman et al. (2009).

https://doi.org/10.5194/wes-2023-2
Preprint. Discussion started: 17 February 2023

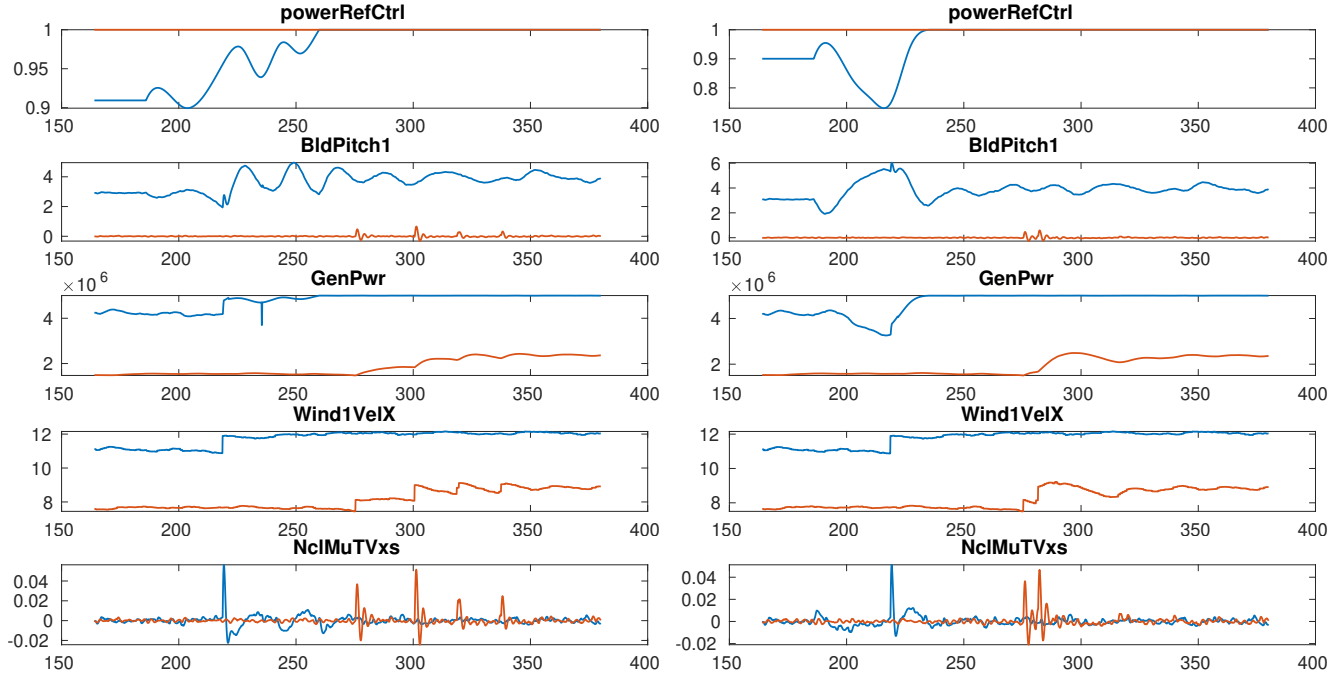

(a) $u_{\mathrm{f,v}} = 1$, $\omega_{\mathrm{T}} = 0$, $\omega_{\mathrm{P}} = 0$ (series 1 case 7).

(b) $u_{\mathrm{f,v}} = 1$, $\omega_{\mathrm{T}} = 100$, $\omega_{\mathrm{P}} = 0$ (series 1 case 8).

Figure 9. Effect of fatigue reduction in optimization result (test series 1 cases 7 and 8).

For optimization we use a module of the self-developed software suite WiFaOpt, which is written in MATLAB. As the optimization requires the simulation it is not a stand-alone program. Therefore, it is unpublished. The optimization method is described in detail in Sect. 2.4.

As data we provide the simulation outputs of baseline and optimization. These outputs are explained in Sect. 3.1 and depicted in App. B. Among them are also those outputs that are used to compute the performance indicators, which are taken into account in the objective function, see Sect. 2.2. These indicators also appear in Tables A1 and A2. Data are available at Zenodo: https://doi.org/10.5281/zenodo.7520546.

Appendix A: Tables

The results of the computational experiments are in Tables A1 and A2, its evaluations in Tables A3–A5 and the summary (of these evaluations) in Table A6. We explain the tables in Sect. 3.1 and discuss them in Sect. 3.2.

https://doi.org/10.5194/wes-2023-2
Preprint. Discussion started: 17 February 2023

eawe european academy of wind energy
Open Access WIND ENERGY SCIENCE DISCUSSIONS

Table A1. Results of test series 1, i.e., pitch activity weight $\omega_P = 0$. The evaluation ratios compare the optimization results to the corresponding baseline results. We explain the table in Sect. 3.1 and discuss it in Sect. 3.2.

Data	Input			Output						Evaluation		
				Baseline			Optimization			Ratios		
Case (No.)	U_{ave} in m s^{-1}	$u_{f,v}$	ω_T	P_b in MW	$a_{T,b}$ in m s^{-1}	$a_{P,b}$ in $^\circ$ s^{-1}	P_o in MW	$a_{T,o}$ in m s^{-1}	$a_{P,o}$ in $^\circ$ s^{-1}	$\frac{P_o}{P_b}$ in %	$\frac{a_{T,o}}{a_{T,b}}$ in %	$\frac{a_{P,o}}{a_{P,b}}$ in %
				U_{ave}: 6, 7, 6–7 m s^{-1}								
1	6	0	0	0.865	0.001	0.000	0.898	0.001	0.000	3.8	9.1	–
1	7	0	0	1.353	0.002	0.000	1.404	0.002	0.000	3.8	6.3	–
1	6–7	0	0	1.200	0.003	0.000	1.226	0.003	0.012	2.2	6.9	–
2	6	0	100	0.865	0.001	0.000	0.884	0.001	0.000	2.2	9.1	–
2	7	0	100	1.353	0.002	0.000	1.404	0.002	0.000	3.8	6.3	–
2	6–7	0	100	1.200	0.003	0.000	1.263	0.003	0.035	5.2	3.4	–
3	6	1	0	0.865	0.001	0.017	0.898	0.001	0.017	3.8	0.0	0.0
3	7	1	0	1.353	0.001	0.021	1.404	0.001	0.020	3.8	-11.1	-2.4
3	6–7	1	0	1.200	0.001	0.032	1.226	0.001	0.040	2.2	8.3	24.9
4	6	1	100	0.865	0.001	0.017	0.896	0.001	0.017	3.6	0.0	-0.6
4	7	1	100	1.353	0.001	0.021	1.402	0.001	0.021	3.6	-11.1	-1.0
4	6–7	1	100	1.200	0.001	0.032	1.200	0.001	0.039	0.0	0.0	20.6
				U_{ave}: 11, 12, 11–12 m s^{-1}								
5	11	0	0	5.488	0.005	0.000	5.657	0.005	0.000	3.1	6.4	–
5	12	0	0	7.460	0.006	0.065	7.460	0.006	0.065	0.0	0.0	0.0
5	11–12	0	0	6.291	0.012	0.077	6.613	0.012	0.071	5.1	-2.4	-7.3
6	11	0	100	5.488	0.005	0.000	5.573	0.005	0.000	1.6	12.8	–
6	12	0	100	7.460	0.006	0.065	7.460	0.006	0.065	0.0	0.0	0.0
6	11–12	0	100	6.291	0.012	0.077	6.785	0.010	0.105	7.9	-18.7	37.3
7	11	1	0	5.488	0.002	0.051	5.657	0.002	0.047	3.1	-9.5	-6.3
7	12	1	0	7.460	0.003	0.098	7.460	0.003	0.098	0.0	0.0	0.0
7	11–12	1	0	6.292	0.005	0.149	6.612	0.005	0.150	5.1	-3.8	0.7
8	11	1	100	5.488	0.002	0.051	5.656	0.002	0.046	3.1	-9.5	-8.9
8	12	1	100	7.460	0.003	0.098	7.460	0.003	0.098	0.0	0.0	0.0
8	11–12	1	100	6.292	0.005	0.149	6.616	0.005	0.133	5.2	-13.5	-10.8
				U_{ave}: 12, 13, 12–13 m s^{-1}								
9	12	0	0	7.482	0.006	0.058	7.482	0.006	0.058	0.0	0.0	0.0
9	13	0	0	8.930	0.006	0.044	8.930	0.006	0.044	0.0	0.0	0.0
9	12–13	0	0	8.227	0.012	0.062	8.227	0.012	0.062	0.0	0.0	0.0
10	12	0	100	7.482	0.006	0.058	7.482	0.006	0.058	0.0	0.0	0.0
10	13	0	100	8.930	0.006	0.044	8.930	0.006	0.044	0.0	0.0	0.0
10	12–13	0	100	8.227	0.012	0.062	8.227	0.012	0.062	0.0	0.0	0.0
11	12	1	0	7.482	0.003	0.091	7.482	0.003	0.091	0.0	0.0	0.0
11	13	1	0	8.930	0.003	0.081	8.930	0.003	0.081	0.0	0.0	0.0
11	12–13	1	0	8.226	0.005	0.119	8.226	0.005	0.119	0.0	0.0	0.0
12	12	1	100	7.482	0.003	0.091	7.482	0.003	0.091	0.0	0.0	0.0
12	13	1	100	8.930	0.003	0.081	8.930	0.003	0.081	0.0	0.0	0.0
12	12–13	1	100	8.226	0.005	0.119	8.226	0.005	0.119	0.0	0.0	0.0

https://doi.org/10.5194/wes-2023-2
Preprint. Discussion started: 17 February 2023

eawe european academy of wind energy
Open Access WIND ENERGY SCIENCE DISCUSSIONS

Table A2. Results of test series 2, i.e., pitch activity weight $\omega_{\mathrm{P}} = 10$. The ratios compare the optimization results to the corresponding baseline results. We explain the table in Sect. 3.1 and discuss it in Sect. 3.2.

Data	Input			Output						Evaluation		
				Baseline			Optimization			Ratios		
Case (No.)	U_{ave} in $\mathrm{m\,s^{-1}}$	$u_{\mathrm{f,v}}$	ω_{T}	P_{b} in MW	$a_{\mathrm{T,b}}$ in $\mathrm{m\,s^{-1}}$	$a_{\mathrm{P,b}}$ in $^\circ\,\mathrm{s^{-1}}$	P_{o} in MW	$a_{\mathrm{T,o}}$ in $\mathrm{m\,s^{-1}}$	$a_{\mathrm{P,o}}$ in $^\circ\,\mathrm{s^{-1}}$	$\frac{P_{\mathrm{o}}}{P_{\mathrm{b}}}$ in %	$\frac{a_{\mathrm{T,o}}}{a_{\mathrm{T,b}}}$ in %	$\frac{a_{\mathrm{P,o}}}{a_{\mathrm{P,b}}}$ in %
U_{ave}: 11, 12, 11–12 $\mathrm{m\,s^{-1}}$												
1	11	0	0	5.488	0.005	0.000	5.657	0.005	0.000	3.1	6.4	–
1	12	0	0	7.460	0.006	0.065	7.363	0.006	0.050	-1.3	-3.3	-24.3
1	11–12	0	0	6.291	0.012	0.077	6.400	0.010	0.047	1.7	-17.1	-39.0
2	11	0	100	5.488	0.005	0.000	5.573	0.005	0.000	1.6	12.8	–
2	12	0	100	7.460	0.006	0.065	7.391	0.006	0.053	-0.9	-1.7	-19.6
2	11–12	0	100	6.291	0.012	0.077	6.643	0.010	0.060	5.6	-17.9	-22.0
3	11	1	0	5.488	0.002	0.051	5.470	0.002	0.047	-0.3	-9.5	-6.5
3	12	1	0	7.460	0.003	0.098	7.365	0.003	0.081	-1.3	-11.8	-16.9
3	11–12	1	0	6.292	0.005	0.149	6.667	0.003	0.091	6.0	-34.6	-38.8
4	11	1	100	5.488	0.002	0.051	5.468	0.002	0.047	-0.4	-9.5	-6.5
4	12	1	100	7.460	0.003	0.098	7.286	0.003	0.077	-2.3	-17.6	-21.6
4	11–12	1	100	6.292	0.005	0.149	6.545	0.003	0.083	4.0	-40.4	-44.4

https://doi.org/10.5194/wes-2023-2
Preprint. Discussion started: 17 February 2023

Table A3. Evaluation of test series 1, i.e., pitch activity weight $\omega_{\mathrm{P}} = 0$. The evaluation ratios compare the optimization results to the associated raw baseline, i.e., always the corresponding baseline without fatigue reduction. We explain the table in Sect. 3.1 and discuss it in Sect. 3.2.

U_{ave}: 6, 7, 6–7 m s^{-1}

Data	Input			U_{ave}: 6 m s^{-1}			U_{ave}: 7 m s^{-1}			U_{ave}: 6–7 m s^{-1}		
Case (No.)	$u_{\mathrm{f,v}}$	ω_{T}	$u_{\mathrm{p,v}}$ opt.	$\frac{P_{\mathrm{o}}}{P_{\mathrm{b,r}}}$ in %	$\frac{a_{\mathrm{T,o}}}{a_{\mathrm{T,b,r}}}$ in %	$\frac{a_{\mathrm{P,o}}}{a_{\mathrm{P,b,r}}}$ in %	$\frac{P_{\mathrm{o}}}{P_{\mathrm{b,r}}}$ in %	$\frac{a_{\mathrm{T,o}}}{a_{\mathrm{T,b,r}}}$ in %	$\frac{a_{\mathrm{P,o}}}{a_{\mathrm{P,b,r}}}$ in %	$\frac{P_{\mathrm{o}}}{P_{\mathrm{b,r}}}$ in %	$\frac{a_{\mathrm{T,o}}}{a_{\mathrm{T,b,r}}}$ in %	$\frac{a_{\mathrm{P,o}}}{a_{\mathrm{P,b,r}}}$ in %
1	0	0	1	3.8	9.1	–	3.8	6.3	–	2.2	6.9	–
2	0	100	1	2.2	9.1	–	3.8	6.3	–	5.2	3.4	–
3	1	0	1	3.8	-36.4	–	3.8	-50.0	–	2.2	-55.2	–
4	1	100	1	3.6	-36.4	–	3.6	-50.0	–	0.0	-58.6	–

U_{ave}: 11, 12, 11–12 m s^{-1}

Data	Input			U_{ave}: 11 m s^{-1}			U_{ave}: 12 m s^{-1}			U_{ave}: 11–12 m s^{-1}		
Case (No.)	$u_{\mathrm{f,v}}$	ω_{T}	$u_{\mathrm{p,v}}$ opt.	$\frac{P_{\mathrm{o}}}{P_{\mathrm{b,r}}}$ in %	$\frac{a_{\mathrm{T,o}}}{a_{\mathrm{T,b,r}}}$ in %	$\frac{a_{\mathrm{P,o}}}{a_{\mathrm{P,b,r}}}$ in %	$\frac{P_{\mathrm{o}}}{P_{\mathrm{b,r}}}$ in %	$\frac{a_{\mathrm{T,o}}}{a_{\mathrm{T,b,r}}}$ in %	$\frac{a_{\mathrm{P,o}}}{a_{\mathrm{P,b,r}}}$ in %	$\frac{P_{\mathrm{o}}}{P_{\mathrm{b,r}}}$ in %	$\frac{a_{\mathrm{T,o}}}{a_{\mathrm{T,b,r}}}$ in %	$\frac{a_{\mathrm{P,o}}}{a_{\mathrm{P,b,r}}}$ in %
5	0	0	1	3.1	6.4	–	0.0	0.0	0.0	5.1	-2.4	-7.3
6	0	100	1	1.6	12.8	–	0.0	0.0	0.0	7.9	-18.7	37.3
7	1	0	1	3.1	-59.6	–	0.0	-43.3	49.2	5.1	-59.3	96.6
8	1	100	1	3.1	-59.6	–	0.0	-43.3	49.2	5.2	-63.4	74.2

U_{ave}: 12, 13, 12–13 m s^{-1}

Data	Input			U_{ave}: 12 m s^{-1}			U_{ave}: 13 m s^{-1}			U_{ave}: 12–13 m s^{-1}		
Case (No.)	$u_{\mathrm{f,v}}$	ω_{T}	$u_{\mathrm{p,v}}$ opt.	$\frac{P_{\mathrm{o}}}{P_{\mathrm{b,r}}}$ in %	$\frac{a_{\mathrm{T,o}}}{a_{\mathrm{T,b,r}}}$ in %	$\frac{a_{\mathrm{P,o}}}{a_{\mathrm{P,b,r}}}$ in %	$\frac{P_{\mathrm{o}}}{P_{\mathrm{b,r}}}$ in %	$\frac{a_{\mathrm{T,o}}}{a_{\mathrm{T,b,r}}}$ in %	$\frac{a_{\mathrm{P,o}}}{a_{\mathrm{P,b,r}}}$ in %	$\frac{P_{\mathrm{o}}}{P_{\mathrm{b,r}}}$ in %	$\frac{a_{\mathrm{T,o}}}{a_{\mathrm{T,b,r}}}$ in %	$\frac{a_{\mathrm{P,o}}}{a_{\mathrm{P,b,r}}}$ in %
9	0	0	1	0.0	0.0	0.0	0.0	0.0	0.0	0.0	0.0	0.0
10	0	100	1	0.0	0.0	0.0	0.0	0.0	0.0	0.0	0.0	0.0
11	1	0	1	0.0	-49.2	55.0	0.0	-54.0	83.6	0.0	-63.4	91.8
12	1	100	1	0.0	-49.2	55.0	0.0	-54.0	83.6	0.0	-63.4	91.8

https://doi.org/10.5194/wes-2023-2
Preprint. Discussion started: 17 February 2023

eawe european academy of wind energy
Open Access WIND ENERGY SCIENCE DISCUSSIONS

Table A4. Evaluation of test series 2, i.e., pitch activity weight $\omega_P = 10$. The evaluation ratios compare the optimization results to the associated raw baseline, i.e., always the corresponding baseline without fatigue reduction. We explain the table in Sect. 3.1 and discuss it in Sect. 3.2.

U_{ave}: 11, 12, 11–12 m s^{-1}													
Data	Input			U_{ave}: 11 m s^{-1}			U_{ave}: 12 m s^{-1}			U_{ave}: 11–12 m s^{-1}		
Case (No.)	$u_{f,v}$	ω_T	$u_{p,v}$ opt.	$\frac{P_o}{P_{b,r}}$ in %	$\frac{a_{T,o}}{a_{T,b,r}}$ in %	$\frac{a_{P,o}}{a_{P,b,r}}$ in %	$\frac{P_o}{P_{b,r}}$ in %	$\frac{a_{T,o}}{a_{T,b,r}}$ in %	$\frac{a_{P,o}}{a_{P,b,r}}$ in %	$\frac{P_o}{P_{b,r}}$ in %	$\frac{a_{T,o}}{a_{T,b,r}}$ in %	$\frac{a_{P,o}}{a_{P,b,r}}$ in %
1	0	0	1	3.1	6.4	–	-1.3	-3.3	-24.3	1.7	-17.1	-39.0
2	0	100	1	1.6	12.8	–	-0.9	-1.7	-19.6	5.6	-17.9	-22.0
3	1	0	1	-0.3	-59.6	–	-1.3	-50.0	24.0	6.0	-72.4	19.5
4	1	100	1	-0.4	-59.6	–	-2.3	-53.3	17.0	4.0	-74.8	8.6

Table A5. Evaluation of test series 1 with regard to the effect of fatigue reduction. The ratios compare the baseline result (exceptionally not optimization) with fatigue reduction to the baseline result without fatigue reduction (which is the associated raw baseline). We explain the table in Sect. 3.1 and discuss it in Sect. 3.2.

U_{ave}: U_ℓ, U_h, U_ℓ–U_h														
Data			Input			U_{ave}: U_ℓ			U_{ave}: U_h			U_{ave}: U_ℓ–U_h		
Case (No.)	U_ℓ in m s^{-1}	U_h in m s^{-1}	$u_{f,v}$	ω_T	$u_{p,v}$ opt.	$\frac{P_b}{P_{b,r}}$ in %	$\frac{a_{T,b}}{a_{T,b,r}}$ in %	$\frac{a_{P,b}}{a_{P,b,r}}$ in %	$\frac{P_b}{P_{b,r}}$ in %	$\frac{a_{T,b}}{a_{T,b,r}}$ in %	$\frac{a_{P,b}}{a_{P,b,r}}$ in %	$\frac{P_b}{P_{b,r}}$ in %	$\frac{a_{T,b}}{a_{T,b,r}}$ in %	$\frac{a_{P,b}}{a_{P,b,r}}$ in %
3	6	7	1	–	0	0.0	-36.4	–	0.0	-43.8	–	0.0	-58.6	–
7	11	12	1	–	0	0.0	-55.3	–	0.0	-43.3	49.2	0.0	-57.7	95.3
11	12	13	1	–	0	0.0	-49.2	55.0	0.0	-54.0	83.6	0.0	-63.4	91.8

Table A6. Summary of test series 1 and 2 evaluation. We only consider scenarios with a wind gust. The ratios have different meanings: They compare the *optimization result* with the associated raw baseline result if the quantity reference is *power*. They compare the *baseline result* with the associated raw baseline result if the quantity reference is *fatigue*. We explain the table in Sect. 3.1 and discuss it in Sect. 3.2.

	Data				Input			Power (P ratio in %)			Tower activity (a_T ratio in %)			Pitch activity (a_P ratio in %)		
Quantity reference	Series	Case(s) (Nos.) to wind speeds			$u_{f,v}$	ω_T	ω_P	U_{ave} in m s^{-1}: 6–7	11–12	12–13	U_{ave} in m s^{-1}: 6–7	11–12	12–13	U_{ave} in m s^{-1}: 6–7	11–12	12–13
power	1	1	5	9	0	0	0	2.2	5.1	0.0	6.9	-2.4	0.0	–	-7.3	0.0
	1	2	6	10	0	100	0	5.2	7.9	0.0	3.4	-18.7	0.0	–	37.3	0.0
	1	3	7	11	1	0	0	2.2	5.1	0.0	-55.2	-59.3	-63.4	–	96.6	91.8
	1	4	8	12	1	100	0	0.0	5.2	0.0	-58.6	-63.4	-63.4	–	74.2	91.8
power	2		1		0	0	10		1.7			-17.1			-39.0	
	2		2		0	100	10		5.6			-17.9			-22.0	
	2		3		1	0	10		6.0			-72.4			19.5	
	2		4		1	100	10		4.0			-74.8			8.6	
fatigue	1	3	7	11	1	–	–	0.0	0.0	0.0	-58.6	-57.7	-63.4	–	95.3	91.8

https://doi.org/10.5194/wes-2023-2
Preprint. Discussion started: 17 February 2023

eawe european academy of wind energy
Open Access WIND ENERGY SCIENCE DISCUSSIONS

Appendix B: Figures

The optimization results of the computational experiments are in Figs. B1–B3 (series 1) and Fig. B4 (series 2). Some sub-figures are repeats (from main part). We explain the figures in Sect. 3.1 and discuss some in Sect. 3.2.

Author contributions. CK and SS deliberated the overarching research goals, wrote the corresponding project proposal, and were responsible for the funding acquisition. FB and RS deduced the intermediate research goals, designed as well as implemented the methodology, and drafted the initial manuscript. FB revised the manuscript for submission.

Competing interests. The authors declare that they have no conflict of interest.

Acknowledgements. The research of the authors was funded by the German Federal Ministry of Education and Research under grant numbers 05M18MBA-MOReNet and 05M18VHA-MOReNet. The authors would like to thank Ole Falkenberg (IAV GmbH)[19], Bastian Ritter (Industrial Science GmbH)[20] and Axel Schild (IAV GmbH) for fruitful discussions about wind turbines and farms.

[19] now with DNV Maritime Software GmbH
[20] now with Wölfel Engineering GmbH + Co. KG.

https://doi.org/10.5194/wes-2023-2
Preprint. Discussion started: 17 February 2023

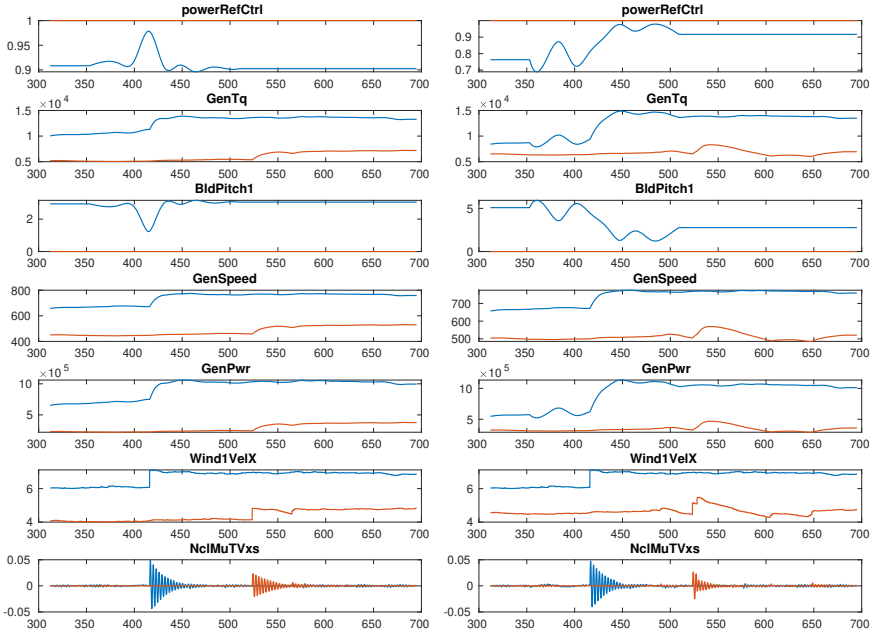

(a) Series 1 case 1 ($u_{\mathrm{f,v}} = 0$, $\omega_{\mathrm{T}} = 0$).

(b) Series 1 case 2 ($u_{\mathrm{f,v}} = 0$, $\omega_{\mathrm{T}} = 100$).

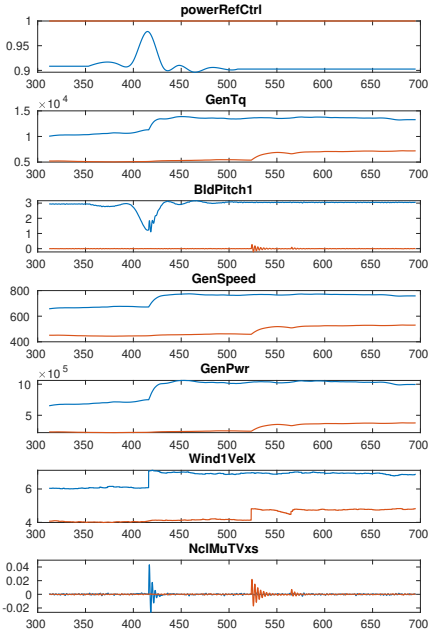

(c) Series 1 case 3 ($u_{\mathrm{f,v}} = 1$, $\omega_{\mathrm{T}} = 0$).

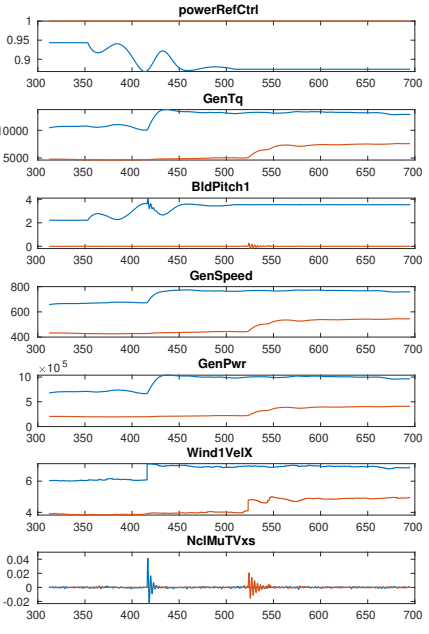

(d) Series 1 case 4 ($u_{\mathrm{f,v}} = 1$, $\omega_{\mathrm{T}} = 100$).

Figure B1. Optimization results of series 1, i.e., pitch activity weight $\omega_{\mathrm{P}} = 0$, cases 1–4, i.e., wind speed of 6–7 $\mathrm{m\,s^{-1}}$. For fatigue reduction $u_{\mathrm{f,v}}$ and tower activity weight ω_{T}, we refer to the sub-captions. We explain the figures in Sect. 3.1.

https://doi.org/10.5194/wes-2023-2
Preprint. Discussion started: 17 February 2023

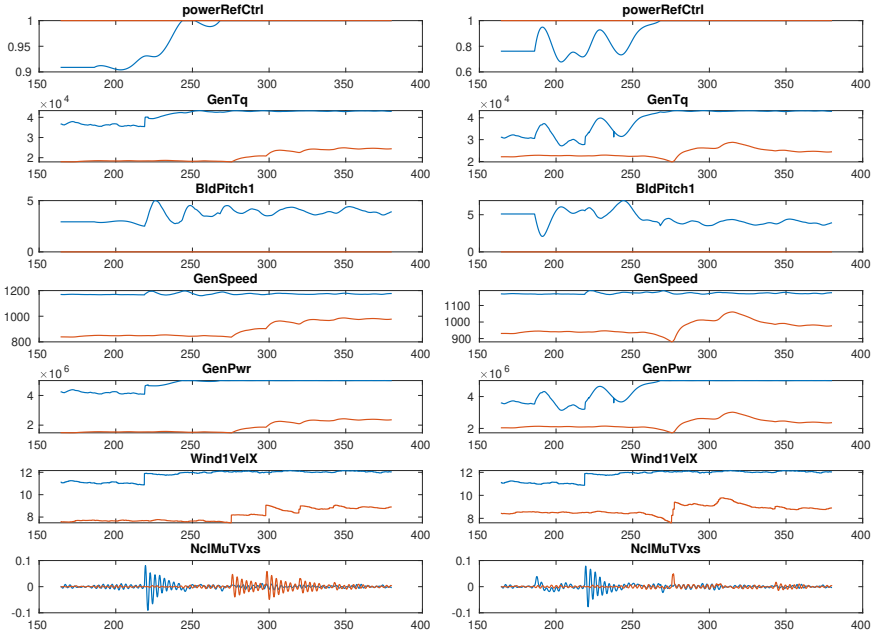

(a) Series 1 case 5 ($u_{\mathrm{f,v}} = 0$, $\omega_{\mathrm{T}} = 0$).

(b) Series 1 case 6 ($u_{\mathrm{f,v}} = 0$, $\omega_{\mathrm{T}} = 100$).

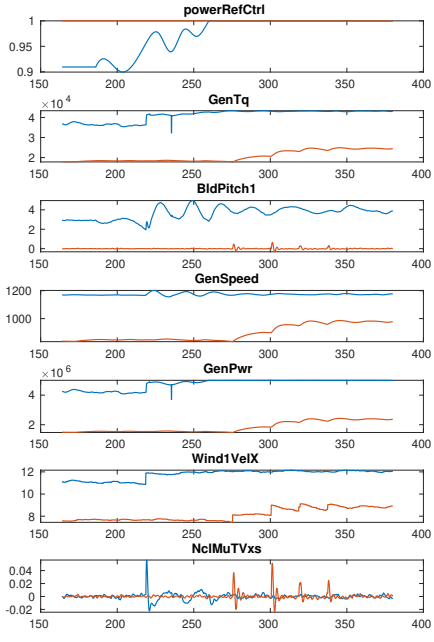

(c) Series 1 case 7 ($u_{\mathrm{f,v}} = 1$, $\omega_{\mathrm{T}} = 0$).

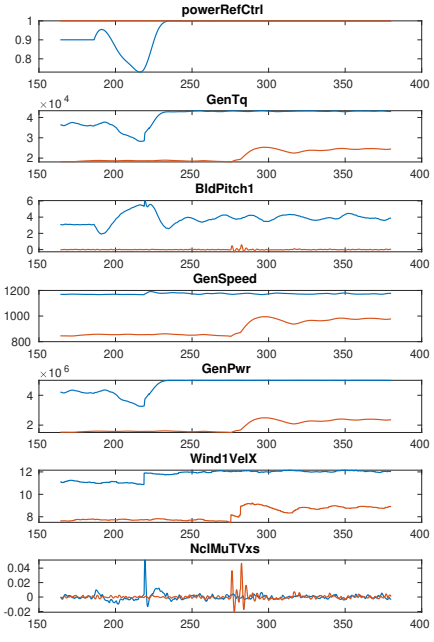

(d) Series 1 case 8 ($u_{\mathrm{f,v}} = 1$, $\omega_{\mathrm{T}} = 100$).

Figure B2. Optimization results of series 1, i.e., pitch activity weight $\omega_{\mathrm{P}} = 0$, cases 5–8, i.e., wind speed of 11–12 $\mathrm{m\,s^{-1}}$. For fatigue reduction $u_{\mathrm{f,v}}$ and tower activity weight ω_{T}, we refer to the sub-captions. We explain the figures in Sect. 3.1.

https://doi.org/10.5194/wes-2023-2
Preprint. Discussion started: 17 February 2023

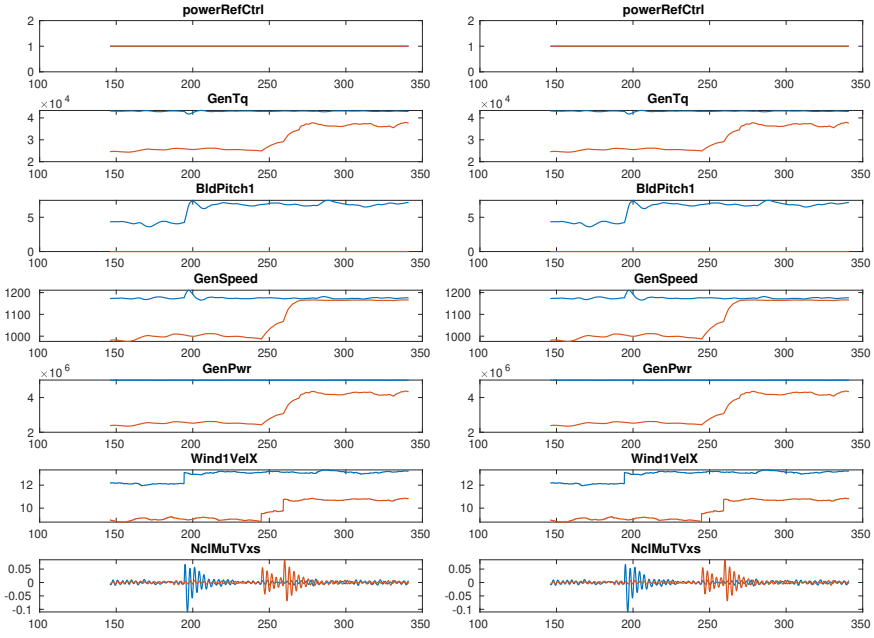

(a) Series 1 case 9 ($u_{\mathrm{f,v}} = 0$, $\omega_{\mathrm{T}} = 0$). (b) Series 1 case 10 ($u_{\mathrm{f,v}} = 0$, $\omega_{\mathrm{T}} = 100$).

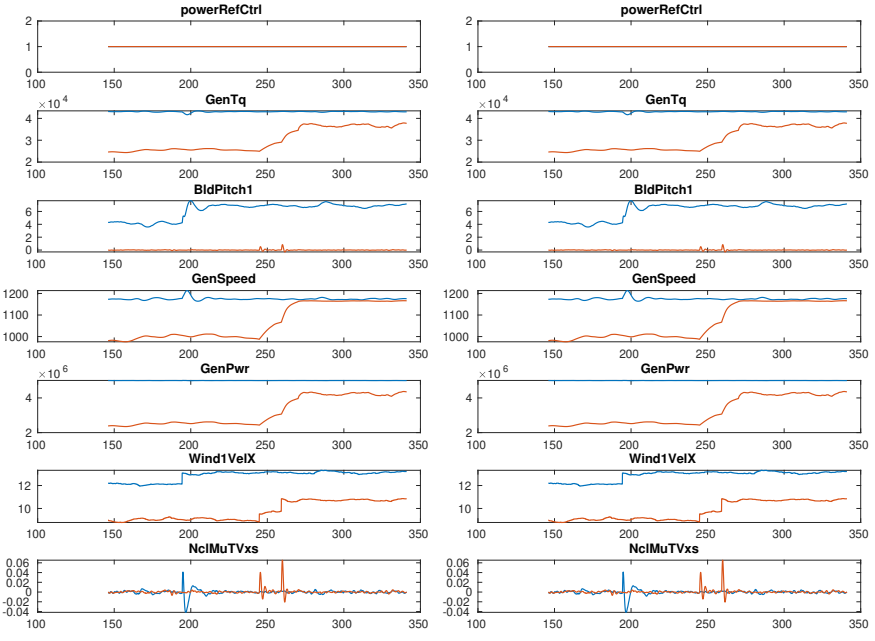

(c) Series 1 case 11 ($u_{\mathrm{f,v}} = 1$, $\omega_{\mathrm{T}} = 0$). (d) Series 1 case 12 ($u_{\mathrm{f,v}} = 1$, $\omega_{\mathrm{T}} = 100$).

Figure B3. Optimization results of series 1, i.e., pitch activity weight $\omega_{\mathrm{P}} = 0$, cases 9–12, i.e., wind speed of 12–13 $\mathrm{m\,s^{-1}}$. For fatigue reduction $u_{\mathrm{f,v}}$ and tower activity weight ω_{T}, we refer to the sub-captions. We explain the figures in Sect. 3.1.

https://doi.org/10.5194/wes-2023-2
Preprint. Discussion started: 17 February 2023

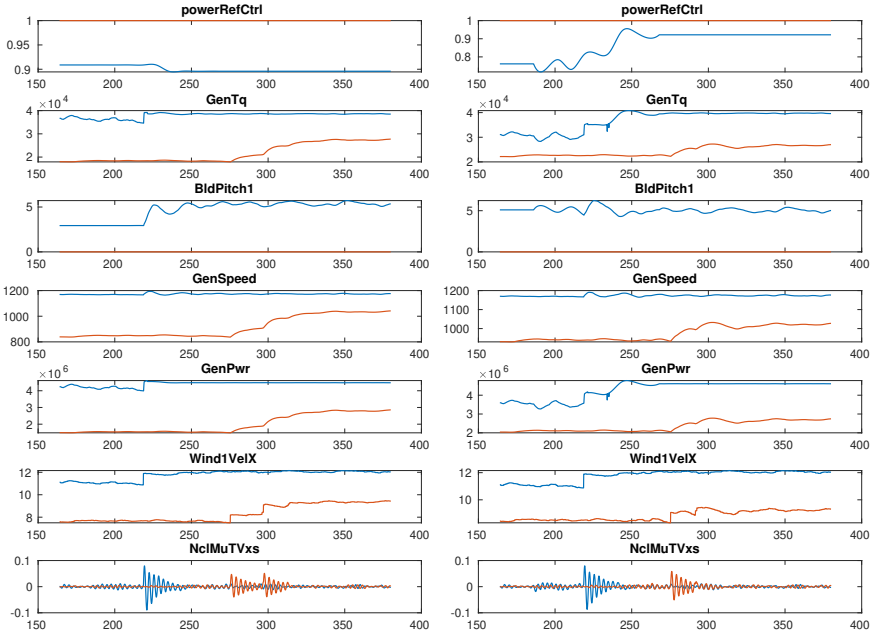

(a) Series 2 case 1 ($u_{\mathrm{f,v}} = 0$, $\omega_{\mathrm{T}} = 0$).

(b) Series 2 case 2 ($u_{\mathrm{f,v}} = 0$, $\omega_{\mathrm{T}} = 100$).

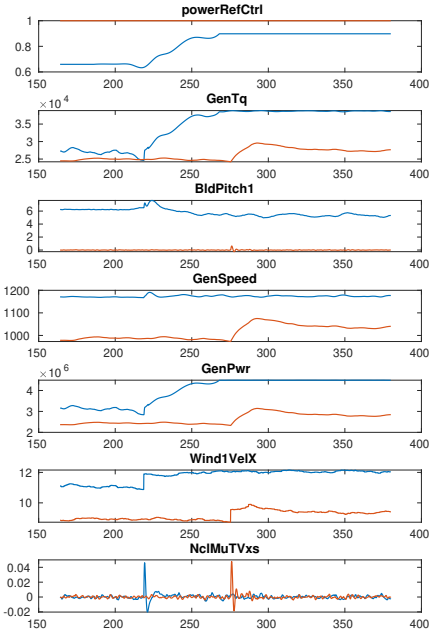

(c) Series 2 case 3 ($u_{\mathrm{f,v}} = 1$, $\omega_{\mathrm{T}} = 0$).

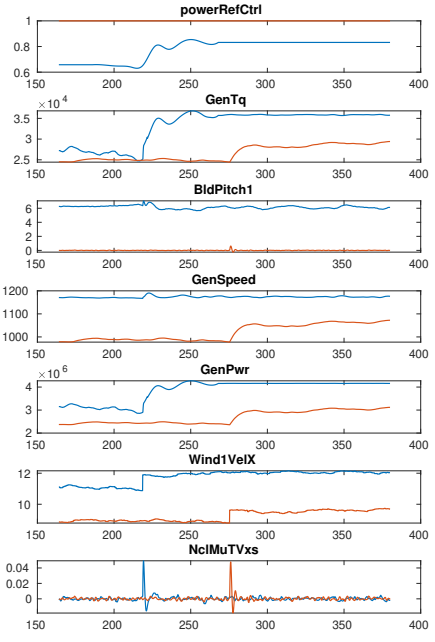

(d) Series 2 case 4 ($u_{\mathrm{f,v}} = 1$, $\omega_{\mathrm{T}} = 100$).

Figure B4. Optimization results of series 2, i.e., pitch activity weight $\omega_{\mathrm{P}} = 10$, cases 1–4, i.e., wind speed of 11–12 $\mathrm{m\,s^{-1}}$. For fatigue reduction $u_{\mathrm{f,v}}$ and tower activity weight ω_{T}, we refer to the sub-captions. We explain the figures in Sect. 3.1.

https://doi.org/10.5194/wes-2023-2
Preprint. Discussion started: 17 February 2023

eawe european academy of wind energy
Open Access WIND ENERGY SCIENCE DISCUSSIONS

References

Annoni, J., Gebraad, P. M. O., Scholbrock, A. K., Fleming, P. A., and van Wingerden, J.-W.: Analysis of axial-induction-based wind plant control using an engineering and a high-order wind plant model, Wind Energy, 19, 1135–1150, https://doi.org/10.1002/we.1891, 2016.

Annoni, J., Fleming, P., Scholbrock, A., Roadman, J., Dana, S., Adcock, C., Porte-Agel, F., Raach, S., Haizmann, F., and Schlipf, D.: Analysis of control-oriented wake modeling tools using lidar field results, Wind Energy Science, 3, 819–831, https://doi.org/10.5194/wes-3-819-2018, 2018.

Bastankhah, M. and Porté-Agel, F.: Experimental and theoretical study of wind turbine wakes in yawed conditions, Journal of Fluid Mechanics, 806, 506–541, https://doi.org/10.1017/jfm.2016.595, 2016.

Ennis, B. L., White, J. R., and Paquette, J. A.: Wind turbine blade load characterization under yaw offset at the SWiFT facility, Journal of Physics: Conference Series, 1037, 052 001, https://doi.org/10.1088/1742-6596/1037/5/052001, 2018.

Fischetti, M. and Pisinger, D.: Mathematical Optimization and Algorithms for Offshore Wind Farm Design: An Overview, Business & Information Systems Engineering, 61, 469–485, https://doi.org/10.1007/s12599-018-0538-0, 2019.

Fleming, P. A., Ning, A., Gebraad, P. M. O., and Dykes, K.: Wind plant system engineering through optimization of layout and yaw control, Wind Energy, 19, 329–344, https://doi.org/10.1002/we.1836, 2016.

Gebraad, P. M. O. and van Wingerden, J.-W.: A Control-Oriented Dynamic Model for Wakes in Wind Plants, Journal of Physics: Conference Series, 524, 012 186, https://doi.org/10.1088/1742-6596/524/1/012186, 2014.

Gebraad, P. M. O. and Wingerden, J.-W.: Maximum power-point tracking control for wind farms, Wind Energy, 18, 429–447, https://doi.org/10.1002/we.1706, 2015.

Gebraad, P. M. O., Teeuwisse, F. W., van Wingerden, J.-W., Fleming, P. A., Ruben, S. D., Marden, J. R., and Pao, L. Y.: A data-driven model for wind plant power optimization by yaw control, in: 2014 American Control Conference, pp. 3128–3134, https://doi.org/10.1109/ACC.2014.6859118, 2014.

Gebraad, P. M. O., Fleming, P. A., and van Wingerden, J.-W.: Comparison of actuation methods for wake control in wind plants, in: 2015 American Control Conference (ACC), pp. 1695–1701, https://doi.org/10.1109/ACC.2015.7170977, 2015.

Gebraad, P. M. O., Teeuwisse, F. W., van Wingerden, J.-W., Fleming, P. A., Ruben, S. D., Marden, J. R., and Pao, L. Y.: Wind plant power optimization through yaw control using a parametric model for wake effects—a CFD simulation study, Wind Energy, 19, 95–114, https://doi.org/10.1002/we.1822, 2016.

Gebraad, P. M. O., Thomas, J. J., Ning, A., Fleming, P. A., and Dykes, K.: Maximization of the annual energy production of wind power plants by optimization of layout and yaw-based wake control, Wind Energy, 20, 97–107, https://doi.org/10.1002/we.1993, 2017.

Hau, E.: Wind Turbines : Fundamentals, Technologies, Application, Economics, Springer, Berlin, 3rd ed. 2013 edn., https://doi.org/10.1007/978-3-642-27151-9, 2013.

Jensen, N. O.: A Note on Wind Generator Interaction, Tech. Rep. 2411, Risø National Laboratory, 1983.

Jonkman, J., Butterfield, S., Musial, W., and Scott, G.: Definition of a 5-MW Reference Wind Turbine for Offshore System Development, Tech. rep., National Renewable Energy Laboratory, https://doi.org/10.2172/947422, 2009.

Katic, I., Højstrup, J., and Jensen, N. O.: A Simple Model for Cluster Efficiency, in: EWEC'86. Proceedings. Vol. 1, edited by Palz, W. and Sesto, E., pp. 407–410, Raguzzi, A., 1987.

https://doi.org/10.5194/wes-2023-2
Preprint. Discussion started: 17 February 2023

Kost, C., Shammugam, S., Jülch, V., Nguyen, H.-T., and Schlegl, T.: Levelized Cost of Electricity : Renewable Energy Technologies, Tech. rep., Fraunhofer Institute for Solar Energy Systems ISE, Freiburg, https://www.ise.fraunhofer.de/content/dam/ise/en/documents/publications/studies/EN2018_Fraunhofer-ISE_LCOE_Renewable_Energy_Technologies.pdf, 2018.

National Renewable Energy Laboratory (NREL): SOWFA: Simulator fOr Wind Farm Applications, https://www.nrel.gov/wind/nwtc/sowfa.html, https://github.com/NREL/SOWFA, accessed: July 2021, 2020.

Platis, A., Siedersleben, S. K., Bange, J., Lampert, A., Bärfuss, K., Hankers, R., Cañadillas, B., Foreman, R., Schulz-Stellenfleth, J., Djath, B., Neumann, T., and Emeis, S.: First *in situ* evidence of wakes in the far field behind offshore wind farms, Scientific Reports, 8, Art. Nr.: 2163, https://doi.org/10.1038/s41598-018-20389-y, 2018.

Zhang, P. Y., Romero, D. A., Beck, J. C., and Amon, C. H.: Solving wind farm layout optimization with mixed integer programs and constraint programs, EURO Journal on Computational Optimization, 2, 195–219, https://doi.org/10.1007/s13675-014-0024-5, 2014.